FLOW CHARACTERISTICS IN A SIMPLE RECIRCULATION SYSTEM

A Thesis Submitted
in partial Fulfilment of the Requirements
for the Degree of
MASTER OF TECHNOLOGY

By
VIJAI PRATAP VERMA

to the

DEPARTMENT OF CIVIL ENGINEERING
INDIAN INSTITUTE OF TECHNOLOGY KANPUR
OCTOBER, 1975

FEB 1976 CE-1975-M-VER-FLO

CERTIFICATE

This is to certify that the thesis entitled 'Flow Characteristics in a Simple Recirculation System' has been carried out under our supervision and the results embodied in this thesis have not been submitted to any other Institute or University for award of a Degree.

Dr. T. Gangadharaiah
Assistant Professor
Dept. of Civil Engineering
Indian Institute of Technology
KANPUR-208016

Dr. K. Subramanya
Professor
Department of Civil Engineering
Indian Institute of Technology
KANPUR-208016

ACKNOWLEDGEMENTS

The author feels it great-pleasure, in expressing his sincere and heartfelt thanks to his supervisors, Dr. T. Gangadharaih and Dr. K. Subramanya, for their valuable guidance and constant encouragement in completion of the thesis work.

I am deeply grateful to Dr. R. Singh, Mechanical Engg. Dept., for his valuable suggestions through extra-ordinary zeal and all possible help at every stage of the work.

I wish to express my sincere thanks to Dr. S. Surya Rao, for suggesting the problem and supervising the work till completion of the experimental set-up.

My thanks are due to Mr. Suresh Kumar, who took too-much pain in getting the experimental set-up ready and to all the staff of Hydraulics Laboratory for their at hand help through-out experimental work.

October, 1975

VIJAI PRATAP VERMA

TABLE OF CONTENTS

LIST OF NOMENCLATURES

A = total area of water flow at a section in cm^2

ΔA = elemental area of water flow in cm^2

b = width of inlet in cm

B = width of the flume in cm

$d, \bar{d}$ = local and width averaged depth in cm

D = maximum width of separation bubble

E_o = energy at inlet

E = energy at any other section except inlet

$h_{o1} - h_{o2}$ = vertical head difference between outer tubes of probe in cm

L_S = length of separation bubble in cm

M_o = momentum at inlet

M = momentum at any other section except inlet

q = local discharge per unit width

q_c = cumulative discharge measured from inside wall

q_{cp} = cumulative discharge at plume center-line

Q = Jet discharge

Q_R = ambient river discharge

R = ratio of initial jet velocity to average ambient velocity

U_o = average velocity of flow at inlet in cm/sec.

Contd. List of Nomenclatures.

U_m = maximum velocity of flow in cm/sec.

v = actual velocity of water flow in the elemental area in cm/sec.

V = initial jet velocity in cm/sec

$\overline{V}_A$ = average ambient velocity in cm/sec.

V_m = mean velocity of flow in cm/sec.

w = unit weight of water

X = distance downstream from inlet in cm

Y = transverse distance from inside wall in cm

α = energy correction coefficient

β = momentum correction coefficient

ϕ = angle between plume center-line and direction of ambient flow, in degrees

ℓ_q = length of zone of flow establishment for jet, measured along plume center-line in cm.

ρ = mass density of water

μ = dynamic viscosity of water.

LIST OF FIGURES

ABSTRACT

Cooling of hot water in a recirculation pond is of very much importance to the industries and thermal power stations. Cooling phenomena is function of diffusion of the flow and the flow characteristics in a recirculation pond. Here an attempt is made to study the flow characteristics in a simple recirculation channel. The flow characteristics studied are the velocity contours at different planes, and decay of maximum velocity, momentum, momentum and energy from the inlet.

The path of maximum velocity behaves as a two-dimensional jet in a cross-flow with velocity equal to the channel flow average velocity. The length of separation bubble is function of depth of flow only. The momentum correction coefficient and energy correction coefficient decrease with the flow length and attain a fairly constant value. The momentum and energy decay faster near the inlet and then remain constant approximately from a distance $X/b = 8.0$. The effect of outlet becomes predominant at X/b 16.0. The effect of inflow and outflow on the main-flow limits to a distance of $X/b = 8.0$. From a distance X/b 8.0 onwards the flow behaves as a normal open-channel flow.

CHAPTER 1

INTRODUCTION AND LITERATURE REVIEW

1.1 INTRODUCTION:

Steam generation of electric power requires rejection of tremendous quantities of waste-heat, typically 58 per cent to 67 per cent of the energy input to the plant, from the generating units to the surroundings. This heat is transferred in the condensers from the low-pressure steam to the cooling water, and then directly to the atmosphere by means of cooling tower, or indirectly through a river, lake, or other large body of water. The method of 'once through' cooling (in which the cooling water is withdrawn from a nearby natural body of water, heated in the condensers, and then returned to the water body) being economically more desirable, requiring relatively cheap and simple structures than the 'Closed loop system' (i.e. cooling ponds, spray ponds, cooling towers) is employed provided the temperature standards set by various regulating agencies can be achieved. Normally submerged outlet or multi-port diffuser systems have been recently utilized in several installations. The heat discharged into a river or other moving water system is advected downstream by the flow.

Being mixed and dispersed within the receiving water, the heat is eventually transferred to the atmosphere by evaporation, radiation or as conduction of sensible heat. There may be some transfer of heat at the soil-water interface due to infiltration of river water into the ground. The amount of heat transferred by diffusion and dispersion in the porous media, however, is generally very small and may be neglected. The temperature distribution downstream from the point of thermal discharge is determined by the hydrodynamic characteristics of the stream and the meteorological conditions prevailing at the site. The first factors determine the advective and turbulent transfer processes within the flow, while the second influence the heat exchange to the atmosphere.

As a first step to understand the thermal characteristics of the diffuser system, it is necessary to know the hydrodynamic features of the flow system. Since the distribution of heat is governed by the velocity distribution, the following investigation was aimed at, for the study of velocity distribution in the recirculating cooling pond. In the present study the flow characteristics resulting from a simple intake-outflow and canal combination is investigated. The object of the study was to determine the velocity distribution, decay

of maximum velocity and diffusion of momentum and kinetic energy near the outlet zone. It is believed that this information would be useful in understanding the thermal behaviour of hot water jet usually encountered in thermal-power station discharges.

1.2 REVIEW OF LITERATURE:

The flow characteristics in a simple recirculation system is considered for review of literature. The flow characteristics include the velocity distribution, temperature and concentration distribution in the flume. In this connection, an extensive work carried out by William W. Sayre (1.0) is reviewed here. Most of the existing methods for predicting the distribution of temperature rises resulting from thermal discharges into aquatic environments are strictly applicable only to large idealized, water bodies, wherein effects of confining channel boundaries are of secondary importance, and throughout which ambient flow properties are constant. But in some cases the complicating factors of channel boundaries and varying flow properties are important and must be taken in to account.

The outfall structure considered by Sayre was a surface jet entering the river from a fixed rectangular slot. This type of structure is among the most economical. He considered

the cross-sectional shape of the channel, the transverse flow distribution and a relatively high velocity in the channel at the plant site and came out with the result that a single point outfall at the bank will be feasible. Two orientations of the jet were considered by him discharge at right angles to the main river flow, and discharge parallel to the main flow. The basic strategy in the case of right-angle discharge was to 'squirt' the jet for enough-out into the main flow so that it mixed with sufficient river water to achieve the required dilution before it was deflected entirely in the downstream direction. The plume trajectory was considered to be dependent on the ratio of the initial cross-channel momentum of the jet to the downstream momentum of the ambient flow. The right-angle jet provided more rapid initial mining and temperature reduction due to dilution, but it carried further out in to the river. In the case of parallel discharge, initial mixing was less rapid and the plume was seen to be confined to a narrower zone closer to the shore. However, it was seen also spreading transversely due to the dispersive mechanisms of the ambient flow.

His report includes one set of relationships developed for the case of a three-dimensional jet with minor bottom boundary effects and another set for the case of a two-dimensional

bottom attached jet. Both sets were applicable in a strict sense only to ambient flows in an idealized rectangular channel. It is helpful to refer to definition sketch for a jet discharging at right-angles in to an ambient-flow as shown in Fig. 1 to fix the variables in mind. Normalized Cumulative discharge was given as

$$\frac{q_c}{Q_R} = \frac{1}{Q_R} \int_0^y q\,dy \qquad (1.1)$$

Here normalized discharge in used for normalized transverse distance y/B across the channel. Use of q_c rather than y as the primary independent variable permitted a simpler mathematical representation of the transverse mixing process in natural channels because it automatically accounted to a considerable extent for variation in flow properties across the channel and for transverse shifts in the ambient flow pattern along the channel. Solutions obtained in the q_c domain can then be transferred to the y domain, if so desired, using equation (1.2) as a mapping function.

Scaling parameter

$$\zeta = 5 \sqrt{bd} \qquad (1.2)$$

Was introduced as the length of the zone of flow establishment, measured along the center-line of the plume. In equation (1.2), b and d are, respectively, the initial jet width and jet height.

He gave the actual relationships for two and three-dimensional jets as follows:

$$\ell_q = 10\ b$$

for two dimensional jet and

$$\ell_q = 3\sqrt{bd}$$

For the three-dimensional jet. Equation (1.2) was used as a compromise between these relationships. It was judged by him that in the case studied the thermal discharge behaved like a three-dimensional jet initially, but as it expanded vertically and encountered the bottom, mixing and entrainment retarded and it began to behave more like a two-dimensional jet. The transition from three-to-two dimensional behaviour occured sooner as discharge and depth decreased. Finally, he used the identity based on continuity.

$$\frac{Q}{Q_R} = \frac{Vbd}{V_A B\bar{d}} \qquad (1.3)$$

As a link between the variables describing the

initial properties of the jet and the corresponding mean properties of the ambient flow. After incorporating Equations 1.1, 1.2 and 1.3, the equations for centerline trajectories were given as follows:

Centerline trajectory for 2-dimensional jet

$$\frac{q_{cp}}{Q_R} = A_1 \left(\frac{X}{\varepsilon_y}\right)^{1/2} \tag{1.4}$$

where $A_1 = \sqrt{2R \frac{Q}{Q_R} \frac{d}{d} \frac{\varepsilon_y}{B}}$ (1.5)

q_{cp} = cumulative discharge of ambient flow at the transverse co-ordinate distance y_p of the centerline and

$R = V/\bar{V}_A$, the ratio of the initial jet velocity to the mean ambient velocity.

Centerline trajectory for 3-dimensional jet

$$\frac{q_{cp}}{Q_R} = A_2 \left(\frac{X}{\varepsilon_y}\right)^{1/3} \tag{1.6}$$

where $A_2 = 0.5372 \frac{\varepsilon_y}{B} R^{2/3}$

The above work deals with decay characteristics of a 3-dimensional jet in a natural river. In this case,

recirculation of water and maintaining temperature do not pose any problem due to vastness of water-system. In a recirculation system the temperature of the circulating water is controlled by diffusion and dissipation of energy flux from the inlet in a small water system. Positioning of an outlet also controls the temperature of the circulating water. It is necessary to know that how far an outlet is to be situated from the inlet for a given channel geometry. The present investigation was carried-out to know a reasonable answer to this question.

CHAPTER II

EXPERIMENTAL INVESTIGATION

2.1 DETAILS OF EXPERIMENTAL SET-UP:

For the experimental study a masonary flume with internal dimensions 870.0 cm x 61.0 cm x 76.0 cm was used. In this two openings 30.5 cm x 30.5 cm for inlet and outlet were made. Centre to centre distance between inlet and outlet was 618.5 cm. Two screens (1.27 cm ϕ holes and 5.08 cm centre to centre) 23.7 cm and 54.2 cm away from inlet are welded in the square conduit (30.5 cm x 30.5 cm) to reduce the fluctuation in the flow. At 22.0 cm away from outlet one adjustable gate was installed to maintain the flow according to requirement. Fig. 2 shows the details of experimental set-up, as shown in it, one reducer 30.5 cm square to 25.4 cm. circular is welded to the square conduit on outlet side, so that it can be connected to 25.4 cm suction pump. On outlet side of pump one gate type valve (22.4 cm) was used to maintain the discharge from pump. After that 20.3 cm circular to 30.5 cm square expansion is used and then 30.5 cm square conduit continues.

Measurement of velocity vector (velocity and direction) was taken by a 3-tube probe and an inclined

(3.88 cm horizontal to 1 cm vertical) manometer. For calibration of the 3-tube probe a glass flume with bottom tappings and a total head tube was used. The total head tube and one bottom tapping of the flume were connected to the manometer after putting it in the direction of flow and at 0.4d (d = depth of flow) from bottom of the flume. It gave almost the same reading as that when an outer and the middle tube of the 3-tube probe were connected to the manometer and was kept in the direction of flow, at 0.4d from bottom of the flume. The above is quite evident from Fig. 3.C. After taking readings in this way, velocity was calculated by using $V = \sqrt{2gh}$ from the total head tube readings. Velocity of the total head tube and corresponding vertical head of the 3-tube probe (difference in readings of the middle and an outer tube in vertical terms) was plotted on log-log paper and best fitting line by least square method was drawn. The best fitting line is called the calibration-curve for 3-tube probe as shown in Fig. 4. To see the angular sensitivity of the 3-tube probe, two velocities one high (78.3 cm/sec.) and the other one low (35.0 cm/sec.) were maintained simultaneously in the glass flume with the bottom tappings. For each case probe was kept at 0.4 d from the bottom of the flume and it was set in such a way, that the manometer reading (when both the

outer tubes were connected to the manometer) came out to be zero. Then probe was moved at 5^{0} interval both ways till it reached 90^{0} and manometer readings were taken for each 5 degrees.

The vertical head on manometer in non-dimensional from $\frac{h_{o1} - h_{o2}}{V_m^2/2g}$ (where V_m is the mean velocity of water flow and $(h_{o1} - h_{o2})$ is head difference in vertical terms when both the outer tubes were connected to manometer) was plotted versus angle moved, which shows the angular sensitivity of the 3-tube probe as shown in Fig. 5.

Tufts of cotton thread were glued at 5 cm distances on the floor of the flume and one thread was attached to point gauge for tracing of separation line at 0.2d, 0.4d and 0.8d from bottom of the flume. Visibility goes on reducing with depth from the surface of water flow. A perpex sheet was allowed to float on the water surface so that the water surface waves are damped and tufts may be made visible clearly.

2.2 RANGE OF EXPERIMENTS CONDUCTED :

Table No. 1.0 gives the range of experiments conducted at 0.215 Froude Number.

TABLE No. 1.0

Experiment No.	Depth of flow	Planes	Sections
1	22.8 cm	0.2d, 0.4d 0.8d	Inlet (9cm away), L/12, L/6, L/3, L/2, 2L/3, 5L/6, 11L/12 outlet (9 cm away).
2	17.1 cm	-do-	-do-
3	8.9 cm	-do-	-do-

Tuft indications at bottom of the flume and at planes 0.2d, 0.4d, 0.8d for the above depth of flows were taken.

2.3 EXPERIMENTAL PROCEDURE:

The flume was filled with water, to a depth slightly greater than 22.8 cms. Circulation of flow in the flume was caused by running the pump. The flow conditions in the flume were maintained at Froude Number 0.215 with depth of flow 22.8 cms. This could be achieved by operation of gate and pump and adding the water to the flume or removing it.

Three tube probe was used to measure the velocity distribution. The probe was aligned in the direction of flow so that the same readings occured in the outer tubes. The direction of flow was measured in angles on the protactor which is mounted on the probe operating device. The velocity head was taken equal to the vertical difference in pressure readings between central and the outer tubes. Equivalent velocity (magnitude) was found by using the calibration curve shown in Fig. 4. In this way readings were taken at many points widthwise and at all the sections and planes selected. In detail these were sections inlet (9 cm away from inner wall), L/12, L/6, L/3, L/2, 2L/3, 5L/6, 11L/12, outlet (9 cm away from inner wall) and planes: 0.2d, 0.4d and 0.8 d from bottom of the flume.

In the same way 17.1 cm and 8.9 cm depth of flow were maintained for 0.215 Froude number. Then readings were taken as explained above. Velocity vectors (magnitude and direction) for each case are shown in Fig. 6.0 (a,b,c).

Details of results are given in Appendices: A1, A2 and A3.

The edge of the separation bubble at each plane (0.2d, 0.4d and 0.8d) was noticed by reversal of orientation of the tufts. The flow-pattern on the bed at upstream

and downstream end of the flume were traced as the tufts indicated and is presented in Figs. 6 (a,b,c) and 7 (a,b,c).

CHAPTER III

ANALYSIS

The experimental results are analysed, viewing the problem as a simple intake-outflow and canal combination. The inflow and outflow of the canal are at right angles to the main flow direction. The characteristics of inflow into the flume, like velocity contour, decay of maximum velocity, decay of momentum and energy are analysed similar to a two-dimensional jet in to a cross flow.

3.1 VELOCITY CONTOURS:

Velocity contours for three-depths of flow (d = 22.8 cm, 17.1 cm and 8.9 cm) and at three planes, i.e. 0.2d, 0.4d and 0.8 d from bottom of the flume for each depth of flow are shown in Fig. 7 (a,b,c). The velocity contours at the inlet and outlet of the flume indicate a good similarity of 2-dimensional jet injection and withdrawal of flow from the flume. The velocity decelerates from inlet of the flume to some distance and accelerates near the out-let of the flume. The length of deceleration and length of acceleration of the flow can be seen very clearly in Fig. 7 (a,b,c). The velocity contours near the inlet curve similar to jet in a cross flow and slowly become

parallel to the main flow. The flow near the outlet indicates similar to withdrawal of flow from the main canal. The velocity contours of the sections near the inlet and outlet indicate a characteristics of maximum velocity in centre of the flow and minimum velocity at the edges.

3.2 SEPARATION BUBBLE :

As the flow enters in to the flume, it separates at the inner side giving rise to separation zone. The line indicating separation bubble from the main flow is shown in Figs. 6 (a,b,c) and 7(a,b,c). Dimensional analysis for the geometry of the separation bubble is carried out below referring to the Fig. 8. Effect of gravity on the geometry of the separation bubble may be neglected, because of the same fluid entering at the same plane into the flume (2). Hence the Froude number effect need not be considered in the analysis. The length of separation bubble should depend on width of the inlet and the flume, depth of flow in the flume, momentum of the inflow and the shear stresses causing the inflow spread. Momentum depends on mass and velocity. Shear stresses are composed of turbulent and viscous components. The first depends on turbulence

intensities which vary with the mean velocity and the latter depends on the fluid viscosity. Therefore, the length of separation bubble can be written as:

$$L_S = f_1 \left[B, b, d, V, \rho, \mu \right] \qquad (3.1)$$

where B = width of the flume

b = width of the inlet

d = depth of flow in the flume

V = velocity of inflow

ρ = mass density of the fluid (water)

and μ = dynamic viscosity of the fluid (water)

By dimensional analysis, Equation (3.1) becomes:

$$\frac{L_S}{b} = f_2 \left(\frac{B}{b}, \frac{d}{b}, \frac{Vd\rho}{\mu} \right) \qquad (3.2)$$

In the cases considered, $\frac{B}{b}$ remains constant and the inflow Reynolds number $\frac{Vd\rho}{\mu}$ is greater than 10^3. At these Reynolds number, the shear stresses causing the inflow spread and leading to the inflow deflection are turbulent. Therefore, the inflow Revnolds number (2) and $\frac{B}{b}$ can be omitted from Equation (3.2), and hence, the length of separation bubble can be represented as:

$$\frac{L_S}{b} = f\left(\frac{d}{b}\right) \quad \ldots \quad \ldots \quad (3.3)$$

Equation (3.3) shows that length of separation bubble depends only on the depth of flow in the flume.

The geometrical characteristics of separation bubble are shown in Fig. 9. Empirical equations to determine the length and maximum width of separation bubble were established in the form

$$L_S/b = -6.45\ d/b + 8.35 \quad (3.4)$$

and $$D/b = 0.55 \quad (3.5)$$

Above equations valid for F = 0.215 and b = 30.45.

Equation (3.4) shows that the length of separation bubble increases with decrease in depth of flow. The ratio L_S/b remains constant across the depth for a particular value of depth of flow, d. Equation (3.5) shows that the maximum width of a bubble is almost constant for 0.2 d, 0.4d and 0.8 d for the values of depth of flow (d = 22.8 cm, 17.1 cm and 8.9 cm).

3.3 ENERGY CORRECTION COEFFICIENT, α AND MOMENTUM CORRECTION COEFFICIENT, β VARIATION:

As a result of non-uniform distribution of velocities over a channel-section, the velocity-head of open channel

flow is generally greater than the value computed according to the expression $V_m^2/2g$, where V_m is the mean velocity.

When energy principle is used in the computation the true velocity head may be expressed as $\alpha V_m^2/2g$, where α is energy correction coefficient or coriolis Coefficient α, can be calculated as follows:

$$\alpha = \frac{\int v^3 \, d\Lambda}{V_m^3 \, \Lambda} \quad \text{or} \quad \frac{\Sigma \, v^3 \, \Delta\Lambda}{V_m^3 \, \Lambda}$$

where Λ = an elementary area

Λ = whole water area

v = actual velocity in the elemental area

and V_m = mean velocity of water flow

Non-uniform distribution of velocities also affects the computation of momentum in open-channel flow. Momentum correction coefficient, β is calculated as follows:

$$\beta = \frac{\int v^2 \, d\Lambda}{V_m^2 \, \Lambda} \quad \text{or} \quad \frac{\Sigma \, v^2 \, \Delta\Lambda}{V_m^2 \, \Lambda}$$

The two velocity-distribution correction coefficients are always slightly larger than the limiting value of unity at which velocity distribution is strictly uniform across the channel section.

The energy and momentum correction coefficients can be as great as 1.6 and 1.2 respectively (3) in channels of complex cross-section. They can vary quite rapidly from section to section in case of irregular alignment. The coefficients are usually higher in steep channels - than in flat channels.

Variation of energy correction coefficient α and momentum correction coefficient, β are shown in Fig. 18 and Fig. 19, respectively. Minimum value of α is 1.06 and its maximum value is 1.87. Value of α increases in all the cases till the section L/12 then decreases up to the section L/3. Afterwards it remains almost same till the section 5L/6 and then once again starts decreasing till it reaches the outlet section. Minimum value of β is 1.027 and its maximum value is 1.27. It behaves in almost the very same way as that of energy correction coefficient.

Increase in energy and momentum correction coefficients at L/12 section is attributed to decrease in inflow area due to separation bubble) and diffusion of inlet-flow in the main-flow.

3.4 LOCATION OF MAXIMUM VELOCITY LINE:

The decay of maximum velocity can be seen clearly in velocity contour diagrams Fig. 7 (a,b,c). The path of

the maximum velocity is traced and plotted in Fig. 12. The decay of maximum velocity at different planes (0.2d, 0.4d, 0.8d from bottom of the flume) for each depth of flow (d = 22.8 cm, 17.1 cm and 8.9 cm) is plotted in Fig. 12(a,b,c). The path of maximum velocity decay remains almost same at different planes (0.2d, 0.4d, 0.8d) for a particular depth of flow, d. The transverse distance Y/b increases with an increase in longitudinal distance X/b initially. In which, Y is distance measured perpendicular to the channel flow from the inlet and X is distance measured in the direction of channel flow from the centre of the inlet. The distance, $\frac{Y}{b}$ of maximum velocity line, from inlet increases till, X/b = 2.5 in longitudinal direction. From X/b = 7.5, Y/b remains almost same and then reduces slightly till, X/b = 18.0. From this section, Y/b goes on reducing till it reaches outlet section, where it is zero.

3.5 DECAY OF MAXIMUM VELOCITY:

Decay of maximum velocity U_m/U_o versus longitudinal distance, X/b (from inlet) is plotted in Fig. 13(a,b,c). This has been derived from velocity contour diagrams (Fig. 7 (a,b,c) from where decay of maximum velocity is seen clearly. The path of maximum velocity decay remains almost same at different planes (0.2d, 0.4d, 0.8d) for a particular depth of flow, d.

For 8.9 cm depth of flow: Maximum velocity is maximum for X/b = 1.0 to 3.0, then it goes on decreasing till X/b = 15.0. From here, it increases till it reaches the outlet section.

For 17.1 cm depth of flow: Maximum velocity is maximum for X/b = 2.5 to 4.5, then it goes on decreasing till X/b = 15.5. From here it increases till it reaches the outlet section.

For 22.8 cm depth of flow: Maximum velocity is maximum for X/b = 1.5 to 4.0, then it goes on reducing till X/b = 16.0. From X/b = 16.0 to 18.0 it remains constant, then increases till it reaches the outlet section.

Hence trend remains almost same in all the cases. The increase in maximum velocity after inlet and near the L/12 section is attributed to decrease in inflow area (due to separation bubble) and diffusion of inflow in the main-flow. Increase in maximum velocity at the outlet is attributed to suction of the outflow..

3.6 DECAY OF MOMENTUM:

The momentum of water passing an elemental area. ΔA per unit time is the product of the mass $wv\,\Delta A/g$ and the velocity v, or $w\,v^2\,\Delta A/g$ (where w = unit wt. of water).

The total momentum of the flow passing a channel section per unit time in $\Sigma w v^2 \Delta A/g$. According to Newton's second law of motion, the change of momentum per unit of time in the body of water in a flowing channel is equal to the resultant of all the external forces that are acting on the body. Momentum is a vector quantity.

Decay of momentum M/M_o (M_o = momentum at inlet section) is plotted against longitudinal distance, X/b from inlet, for each depth of flow (d = 22.8 cm, 17.1 cm and 8.9 cm) in Fig. 15. From the figure it is quite evident that for 17.1 cm depth of flow, the dissipation of momentum near the inlet is faster than that of the other two cases. Once again near the outlet, momentum of 17.1 cm depth of flow increases much faster than the other cases. In all the cases momentum decreases till the longitudinal distance X/b =16.5 and then it starts increasing till it reaches the outlet.

3.7 DECAY OF ENERGY

Assuming ΔA to be an elementary area in whole water area A, and w the unit weight of water. Then the weight of water passing ΔA per unit time with a velocity v is $wv\Delta A$. The kinetic energy of water passing ΔA

per unit time is $wv^3 \Delta A/2g$. This is equivalent to the product of the weight w v ΔA and the velocity head $V^2/2g$. Total kinetic energy passing a channel section (for the whole water area) is equal to Σ w $v^3 \Delta A/2g$. In Open channel flow, for a particular plane, pressure and static energy remains constant, hence only kinetic energy has been considered to show the decay of energy. Energy is a scalar quantity.

Decay of energy E/E_0 (E_0 is energy at inlet section and E at any other section) is plotted against longitudinal distance, X/b from inlet, for each depth of flow (d = 22.8 cms, 17.1 cms and 8.9 cms) in Fig. 15. From the Fig. 15 it is clear that for 17.1 cms depth of flow, the dissipation of energy near the inlet and again the increase of energy near the outlet is much faster than the other two (d=22.8 cm and d= 8.9 cm) cases. Energy remains almost same from X/b = 10.0 to 15.0 for 8.9 cm depth of flow, from X/b = 12.0 to 16.0 for 17.1 cm depth of flow, and from X/b = 15.0 to 18.0 for 22.8 cm depth of flow. Increase of energy, as described above is ofcourse a result of the reduction of depth near the outlet. Elsewhere depth is almost constant.

CHAPTER IV

CONCLUSIONS AND RECOMMENDATIONS

4.1 CONCLUSIONS:

The flow characteristics, in a simple recirculation system is considered here for a preliminary investigation. This problem has good practical application in cooling of hot water, in recirculation ponds, which are very much used by industries. This study is aimed to know the flow characteristics, in a simple recirculation channel, which may be used to predict the length of channel required to attain the normal channel flow characteristics.

The following are the significant conclusions arrived from this study:

1. The plan of the velocity contours give a good visualisation of the flow pattern occuring in a simple recirculation channel.

2. The velocity distribution and path of the maximum velocity of the inflow, behaves as a two-dimensional jet in a cross-flow with velocity equal to the channel flow average velocity. The path of the maximum velocity curves initially due to suction pressure exerted on the inflow. It sticks very near to the outer side (around Y/b =1.5) for greater

part of the channel length ($8.0 < \frac{X}{b} < 16.0$). Near the outlet section, it curves again due to suction offered to the flow. The maximum velocity decays faster for top plane of the flow in comparision with the bottom plane.

3. The length of separation bubble is function of depth of flow only. The variation in length is given by $L_s/b = -6.45 \frac{d}{b} + 8.35$ and maximum width by $D/b = 0.55$.

4. The momentum correction factor, β and energy correction factor, α are found to have large values, $\alpha \simeq 1.6$ and $\beta \simeq 1.25$ near the inlet section. They start decreasing with the flow length and attain a fairly constant value, $\alpha = 1.3$ and $\beta = 1.15$.

5. Momentum decays faster initially up to $X/b = 10.0$, and between $X/b = 10.0$ to 16.0, the flow behaves as sort of uniform flow. From $X/b = 16.0$ onwards the effect of suction becomes predominant. The effective length required to attain the normal open-channel flow characteristics is $X/b = 10.0$. The similar behaviour of decay and uniformness in energy has been found.

4.2 RECOMMENDATIONS:

Based on the investigations carried, the following further studies are recommended:

(1) Variation of the Froude number should be considered.

(2) Variation of the geometry of the inlet and outlet with respect to the channel, with different angle of exit and entrance and different slope of channel should be considered for generalization of the flow.

(3) An intake arrangement constisting of continuous flow in the channel and part of it being used for recirculation will represent a good natural river model.

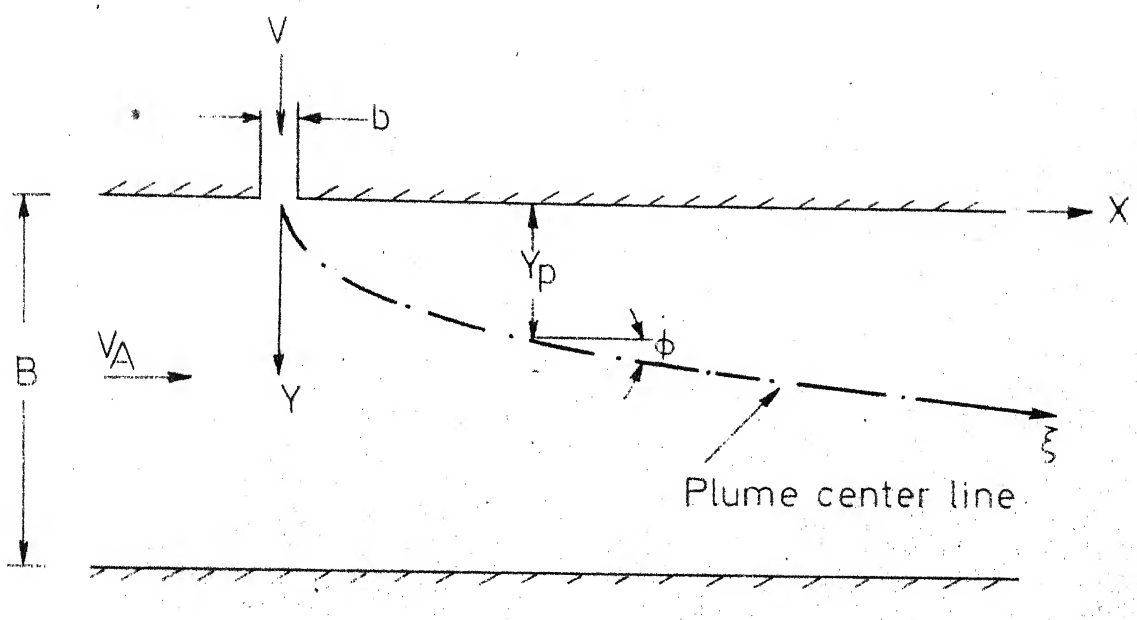

FIG.1 DEFINITION SKETCH FOR JET DISCHARGING AT RIGHT ANGLE IN TO AMBIENT FLOW

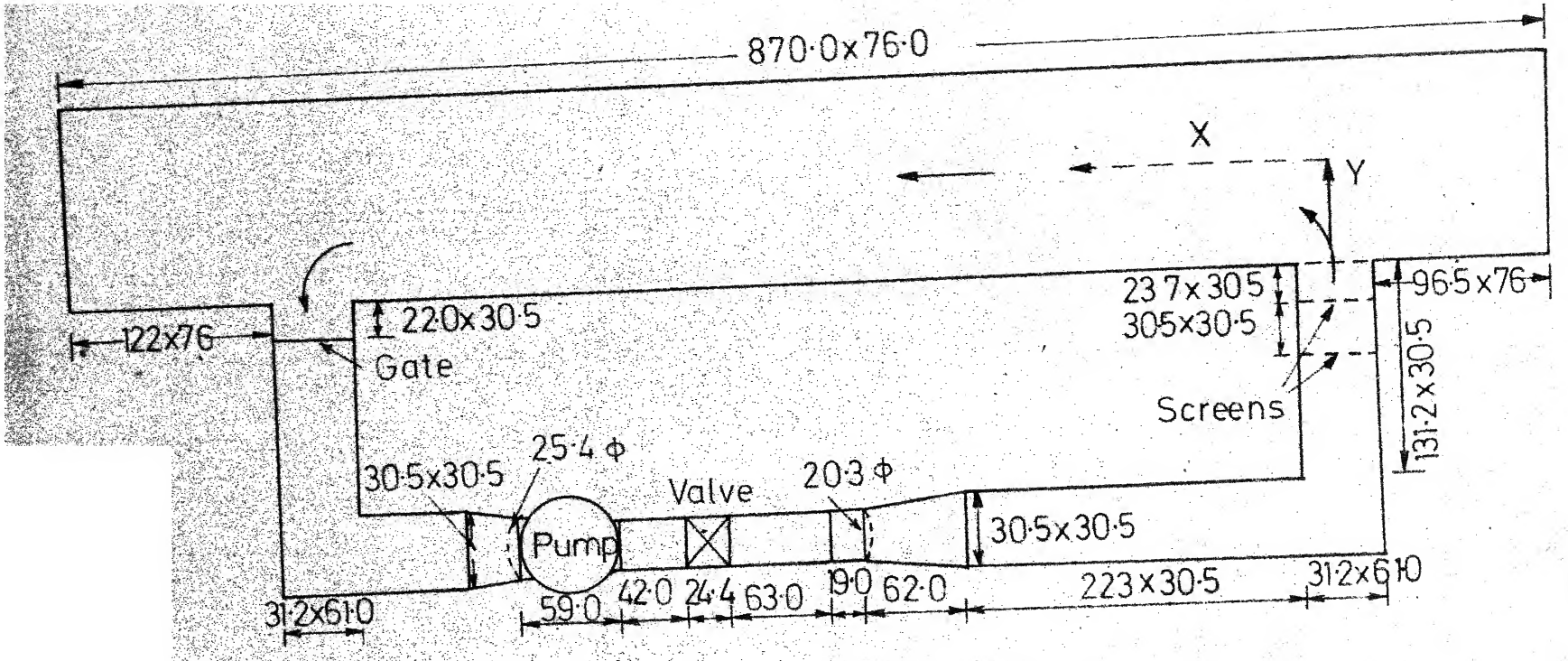

FIG·2 SCHEMATIC DIAGRAM OF SET UP (All dimensions in cm)

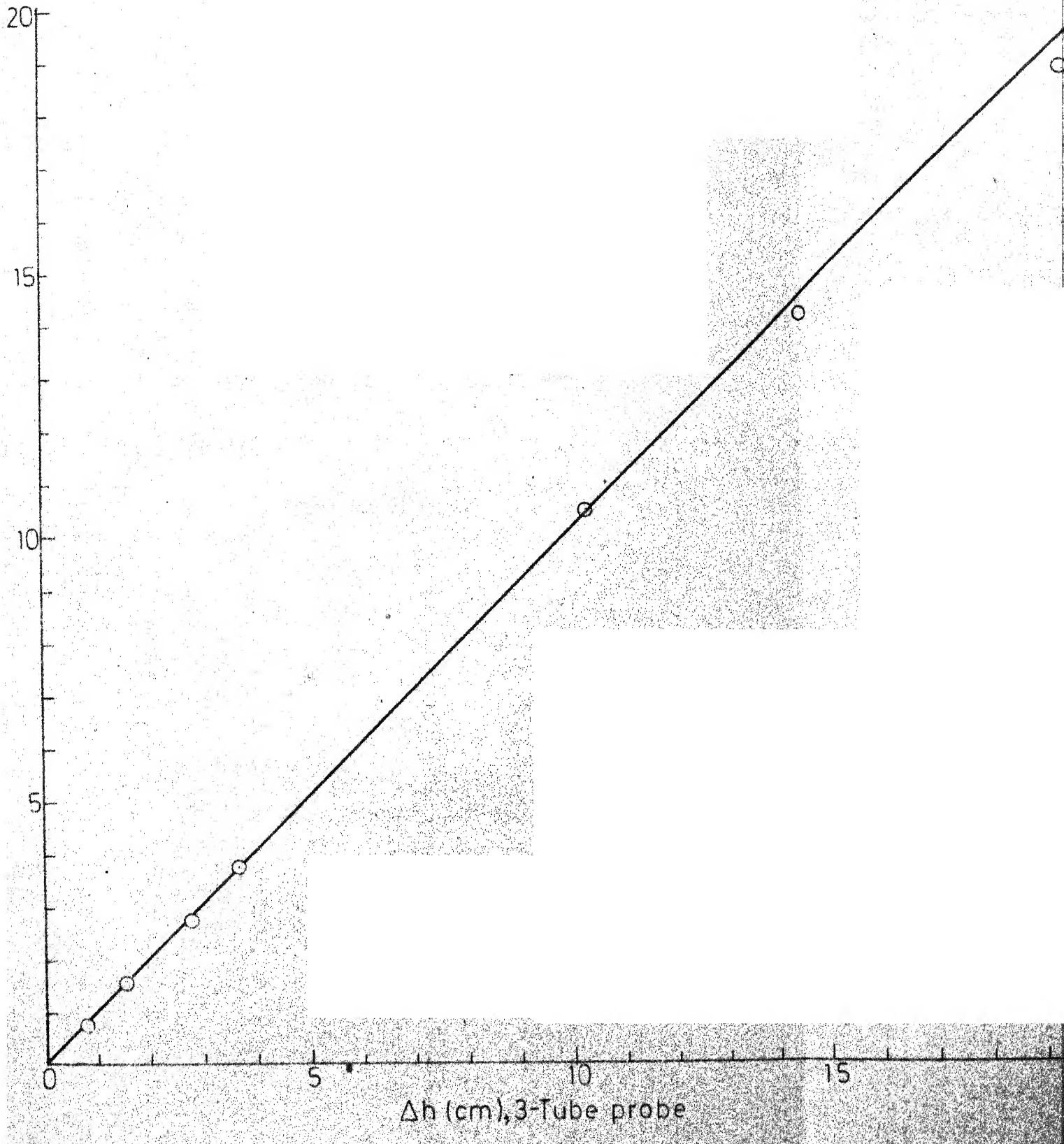

FIG. 3 COMPARISON BETWEEN 3-TUBE PROBE AND TOTAL HEAD TUBE

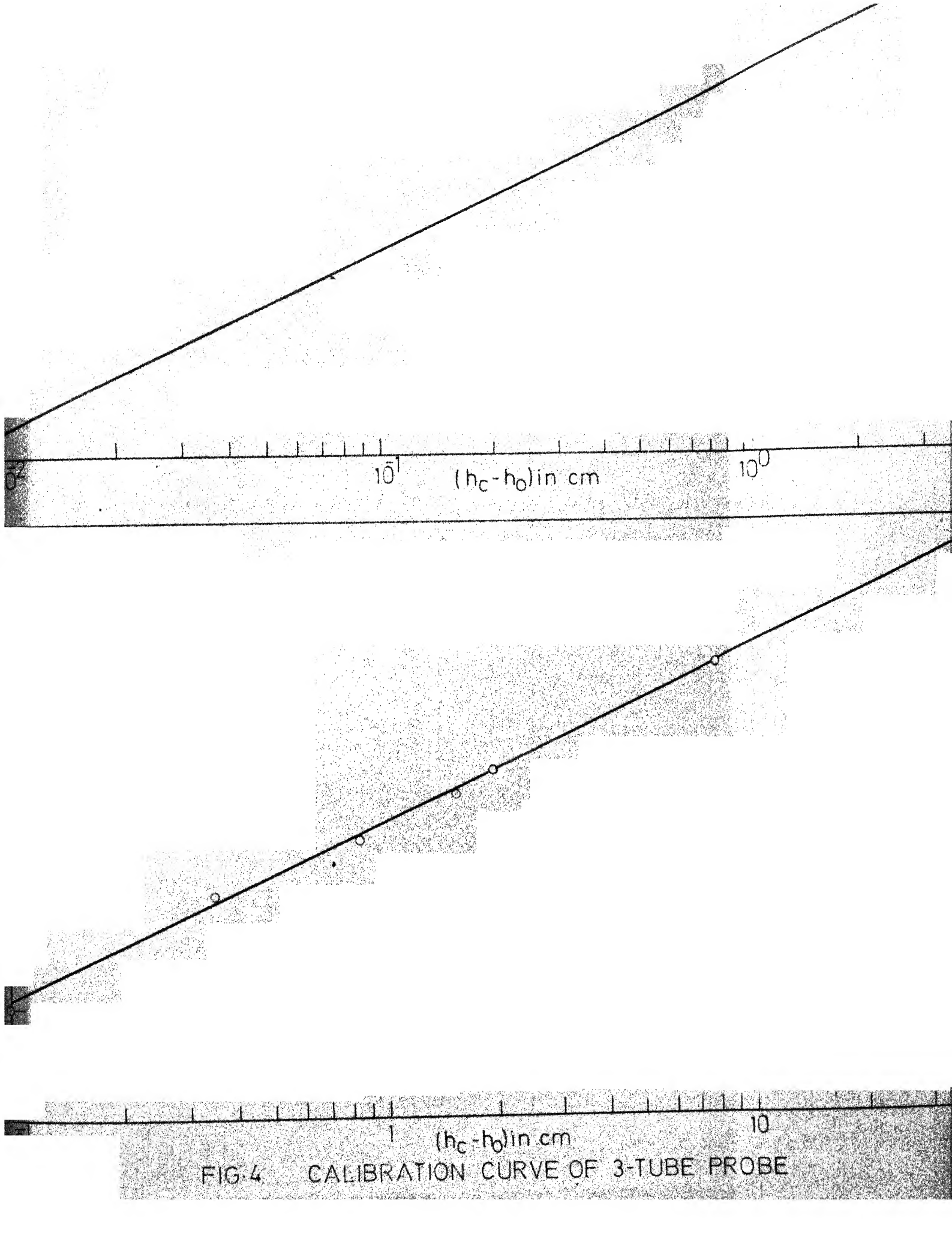

FIG. 4. CALIBRATION CURVE OF 3-TUBE PROBE

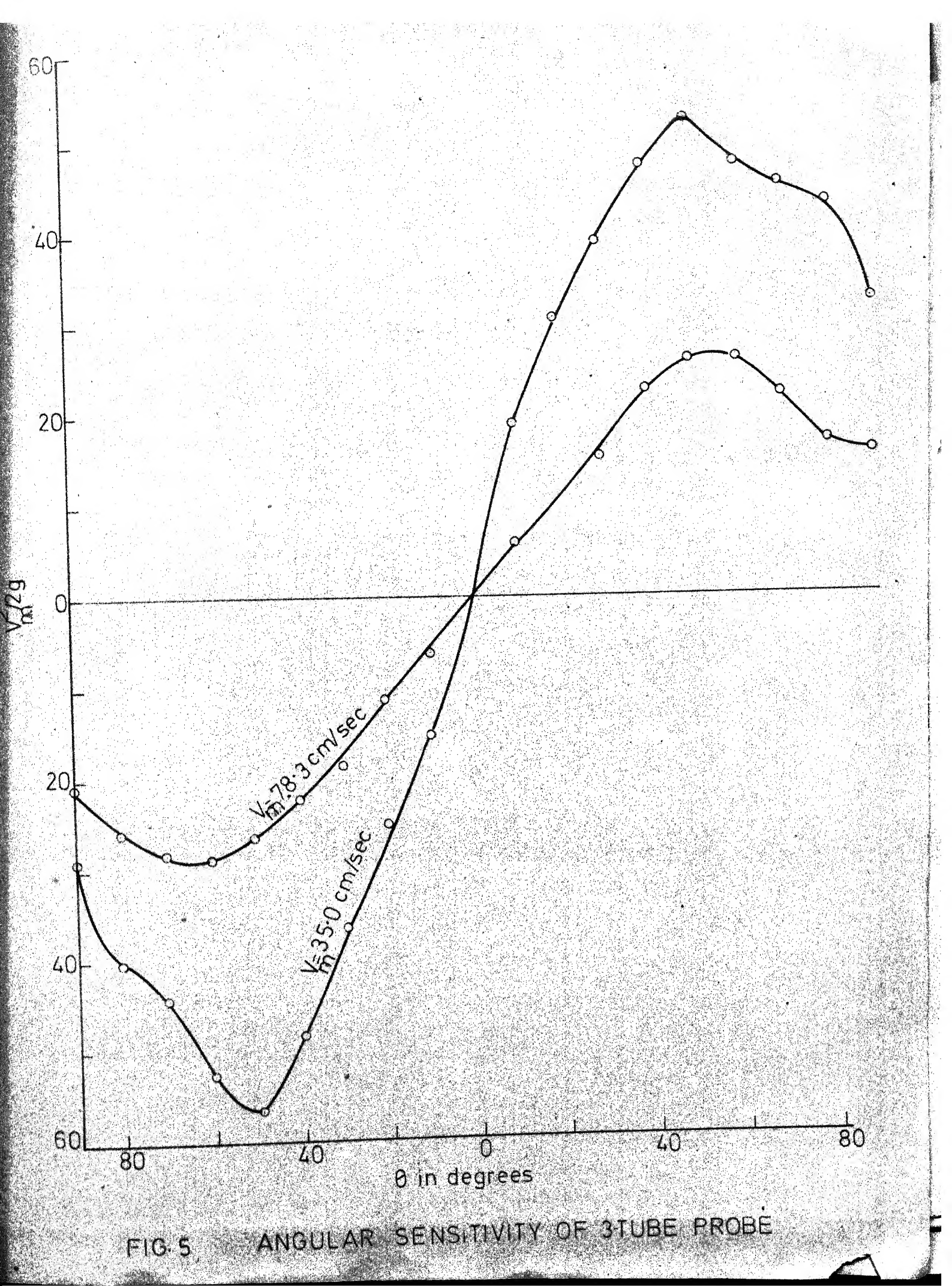

FIG. 5 ANGULAR SENSITIVITY OF 3-TUBE PROBE

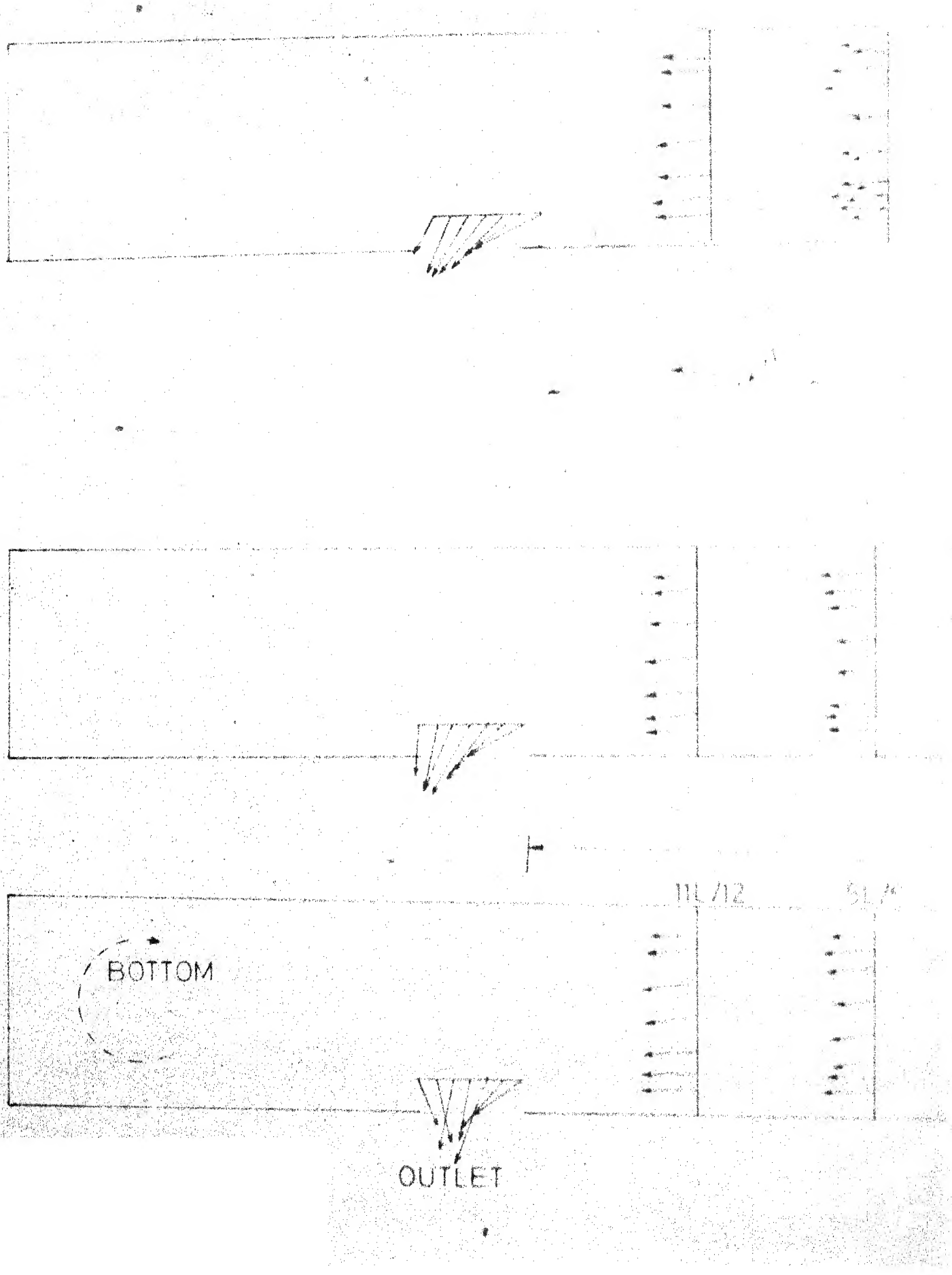

FIG

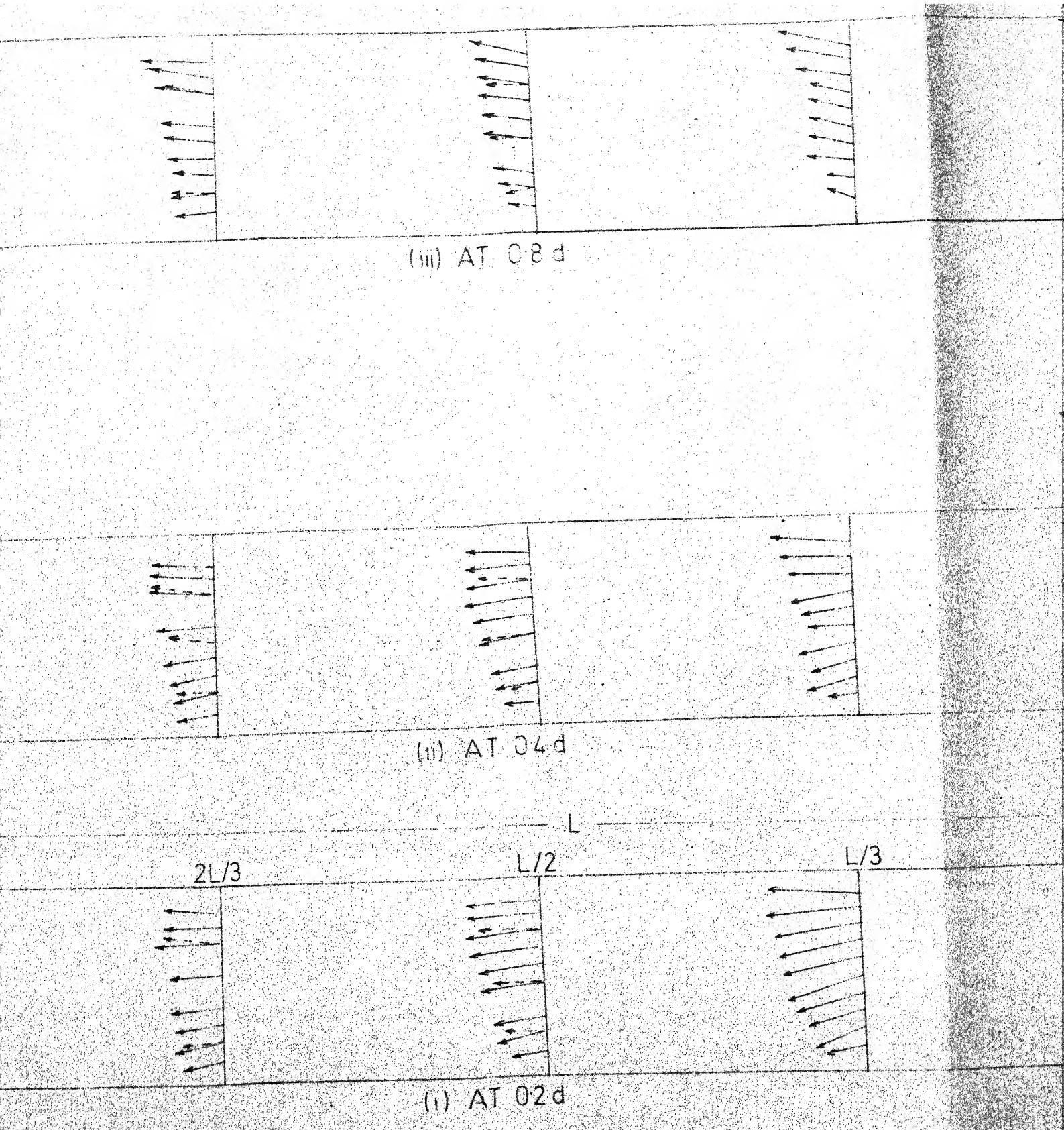

IG. 6(a) VECTOR REPRESENTATION OF VELOCITY

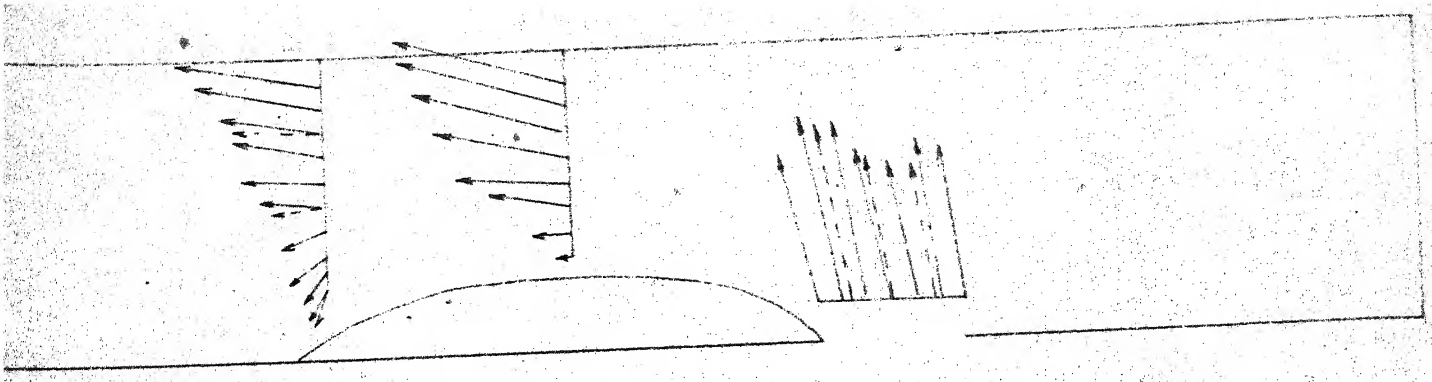

SCALE: 1 CM = 20·0 CMS/SEC

DEPTH OF FLOW 22·8 CMS (9 INCHES)

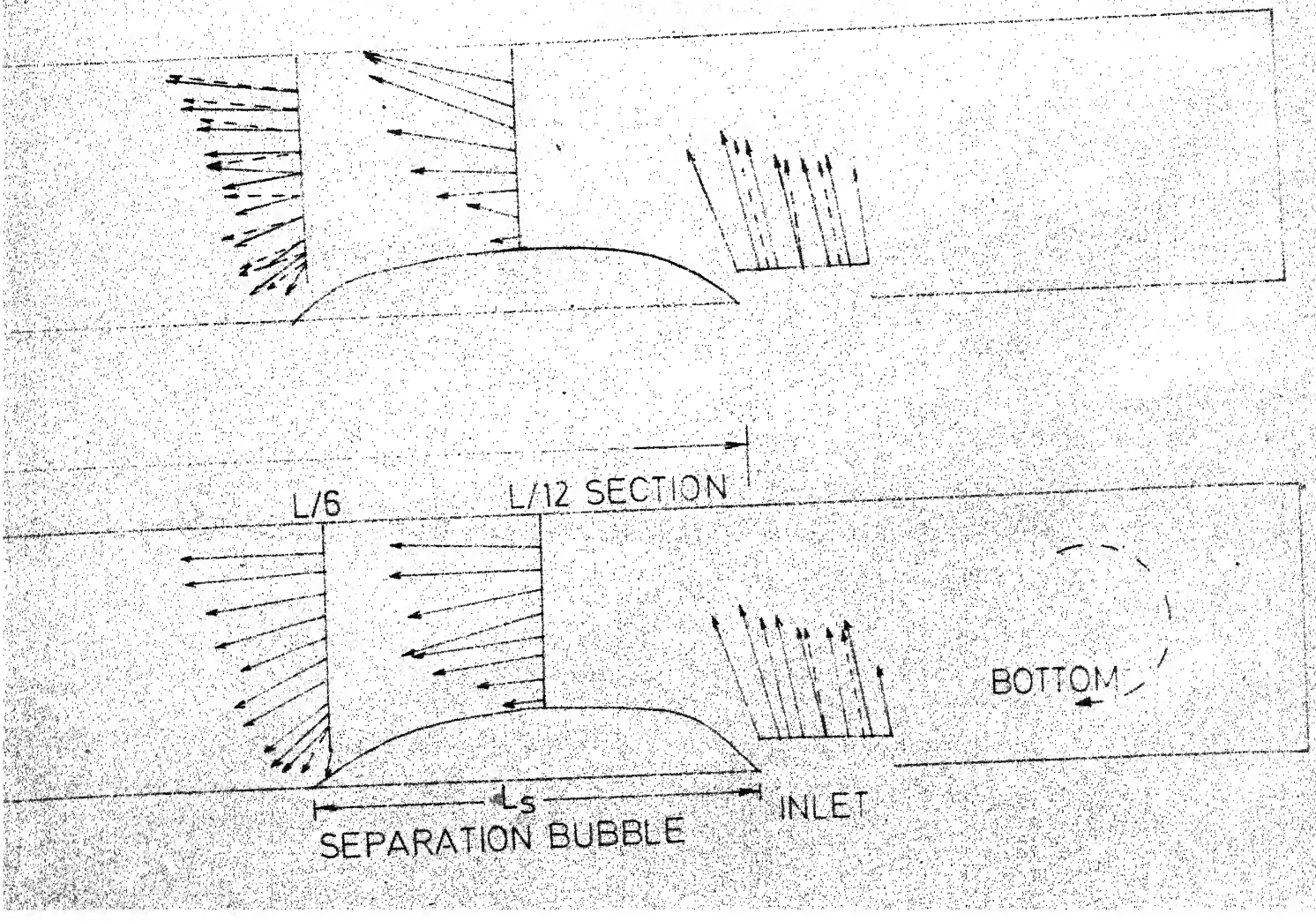

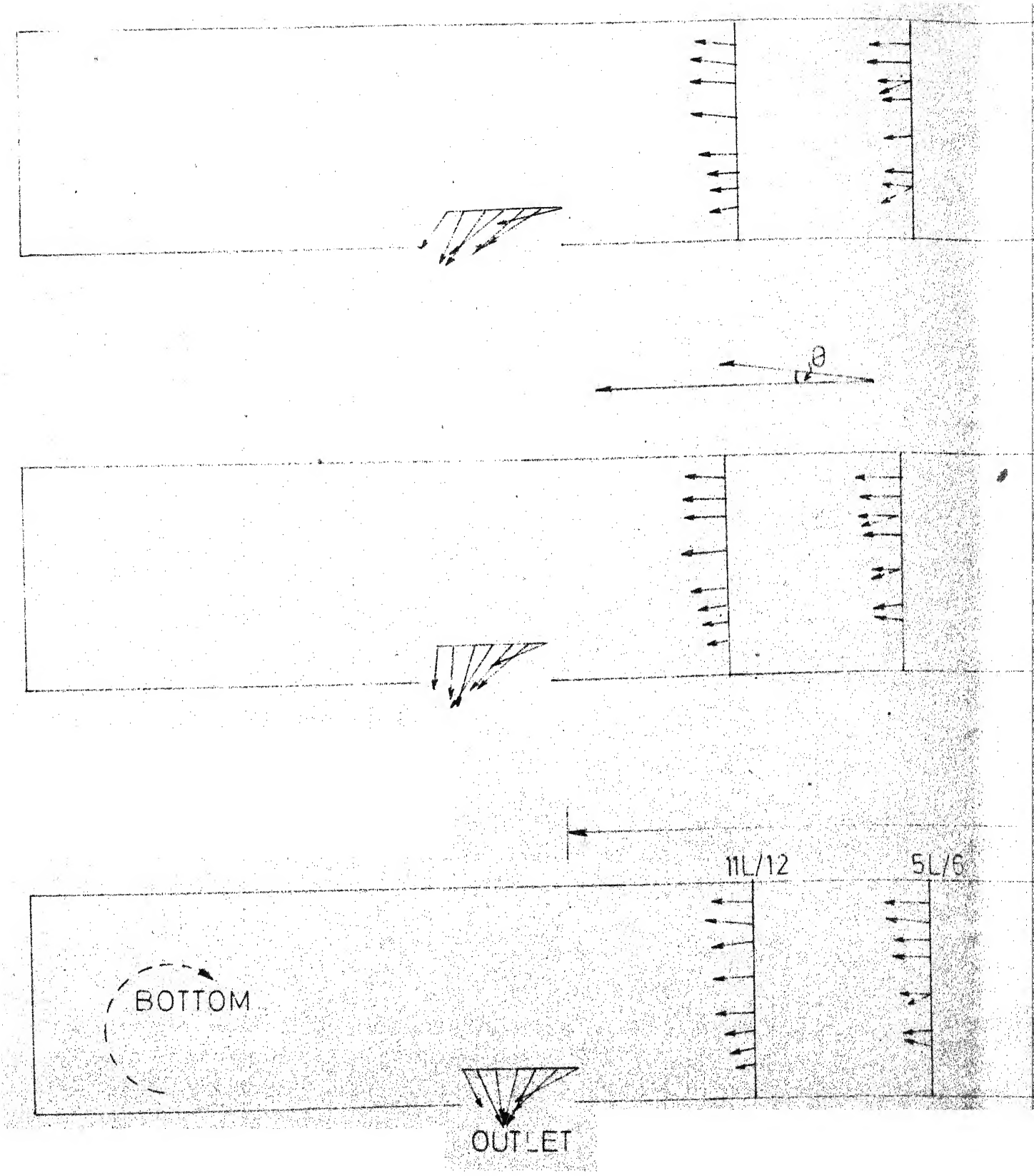
θ
11L/12
5L/6
BOTTOM
OUTLET

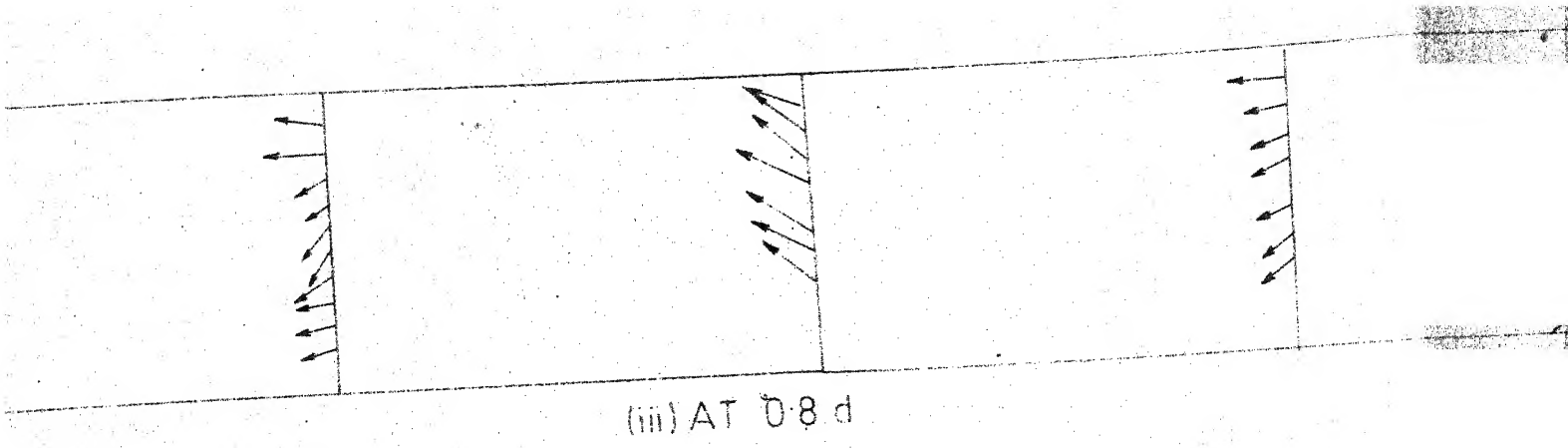

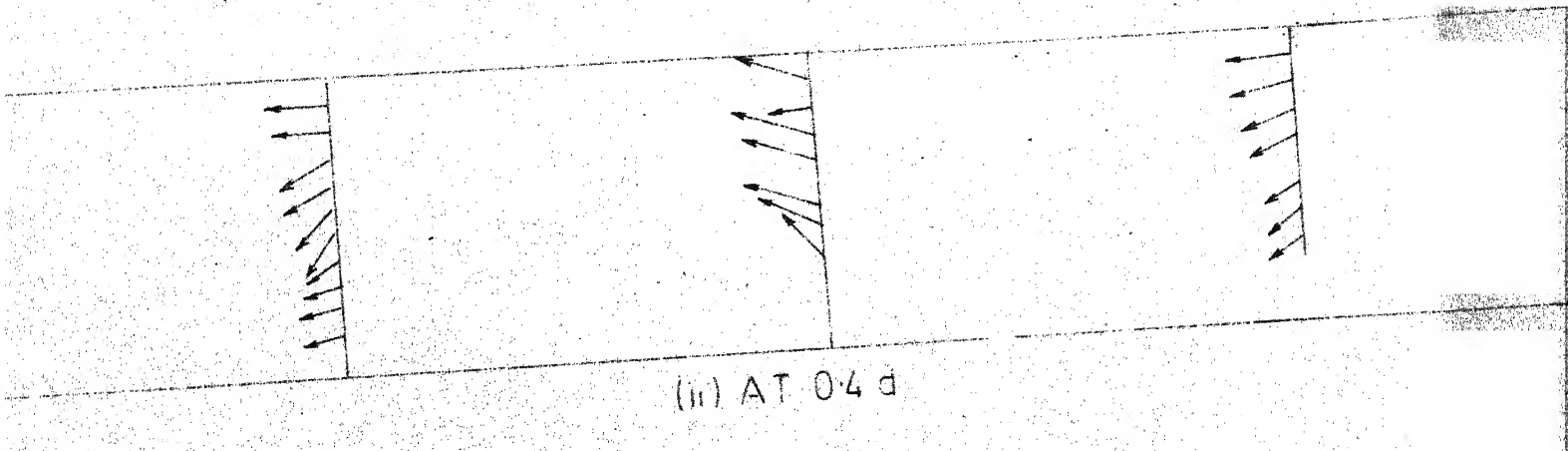

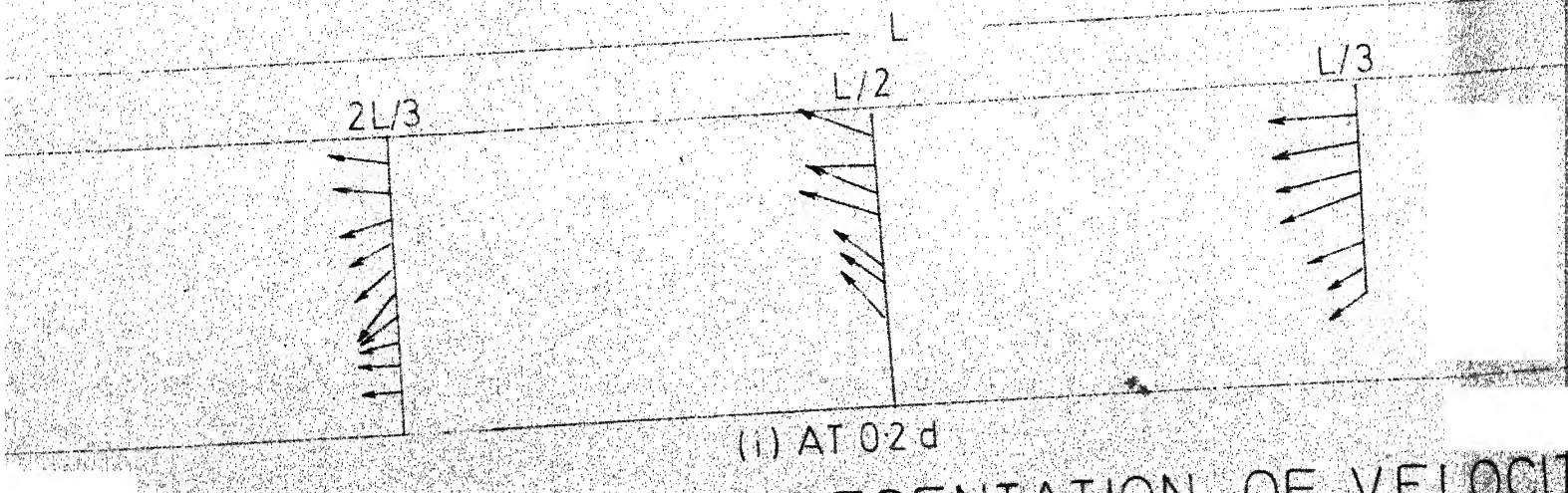

FIG·6(b) VECTOR REPRESENTATION OF VELOCI

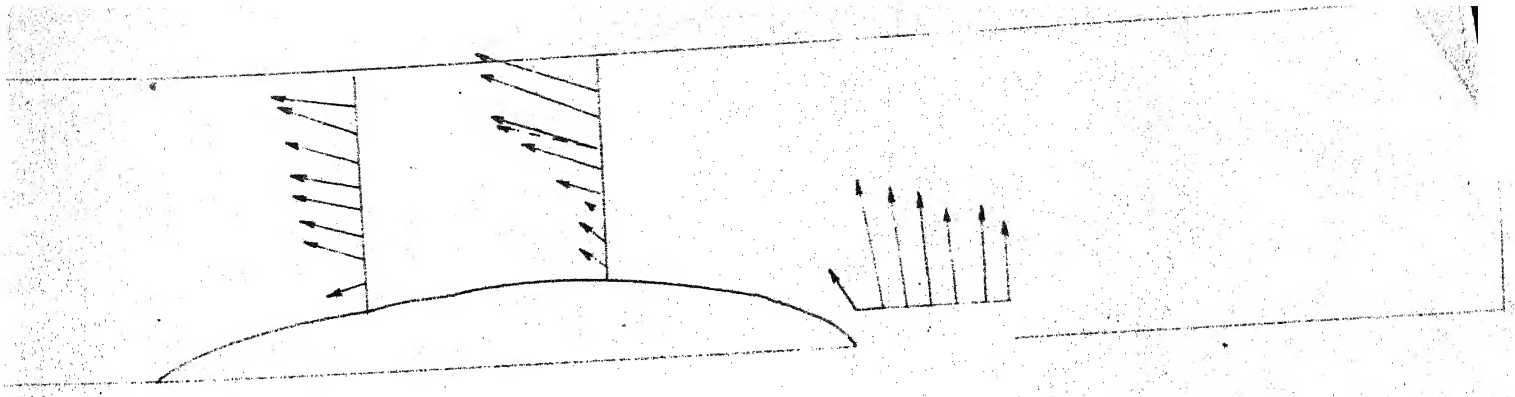

SCALE: 1 CM = 20·0 CMS/SEC

DEPTH OF FLOW 17·1 CMS (6·75 INCHES)

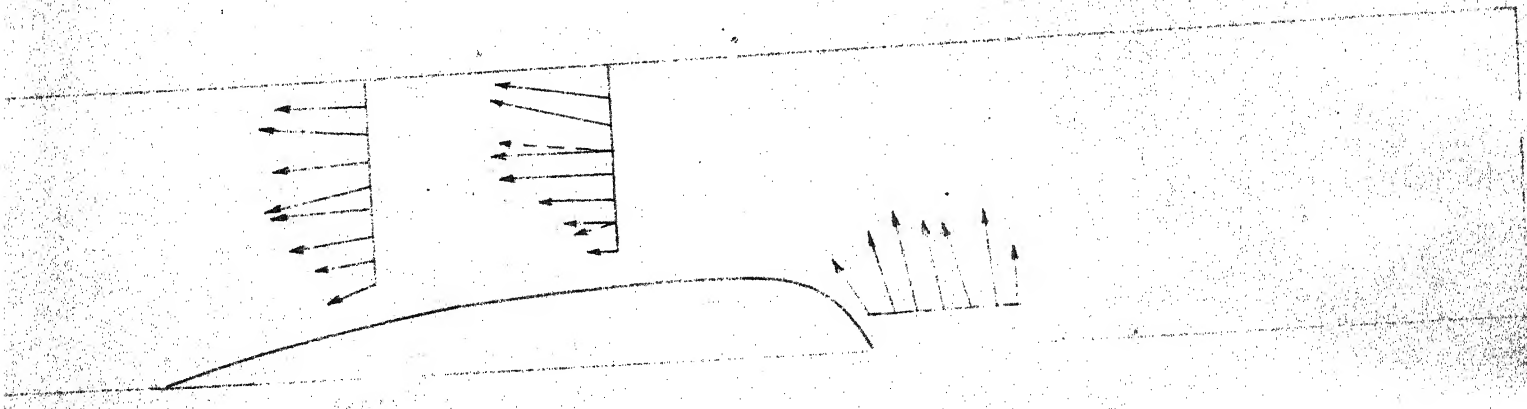

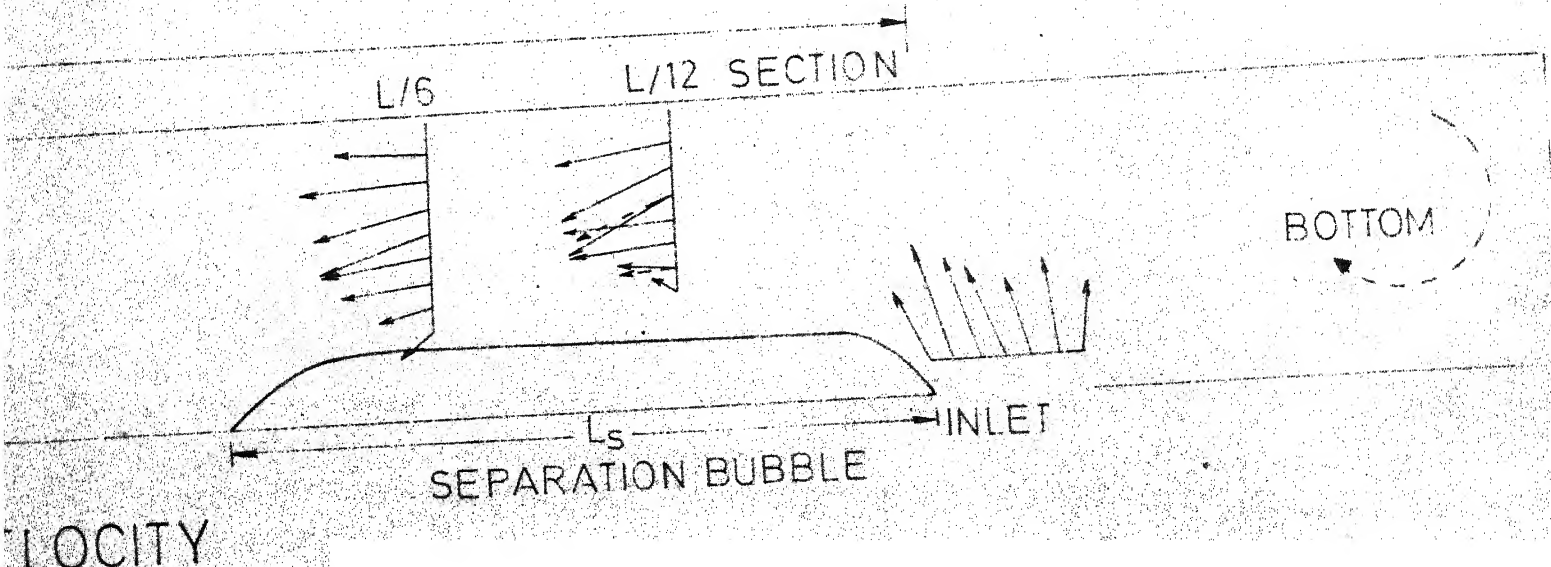

LOCITY

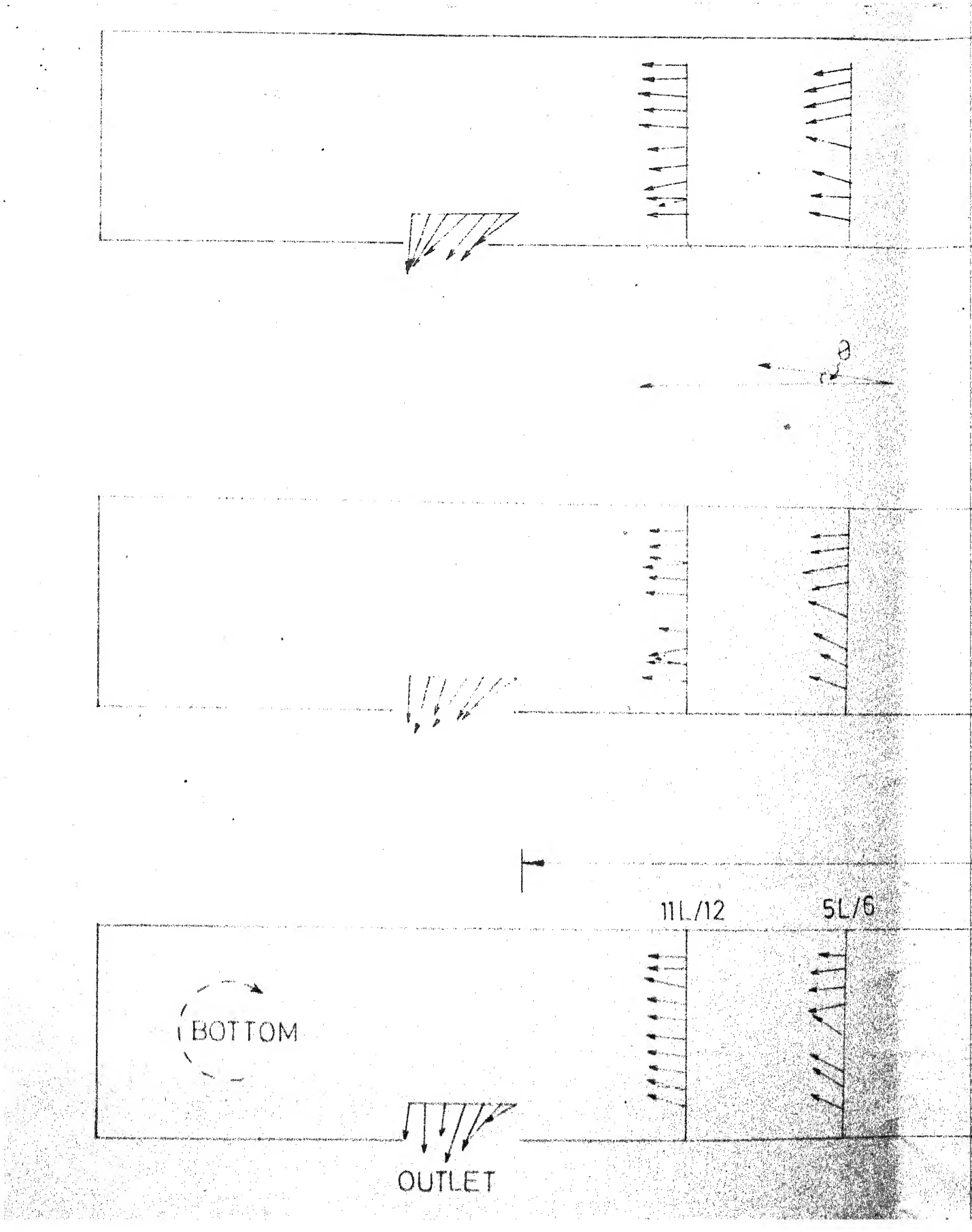
r
θ
11L/12
5L/6
BOTTOM
OUTLET

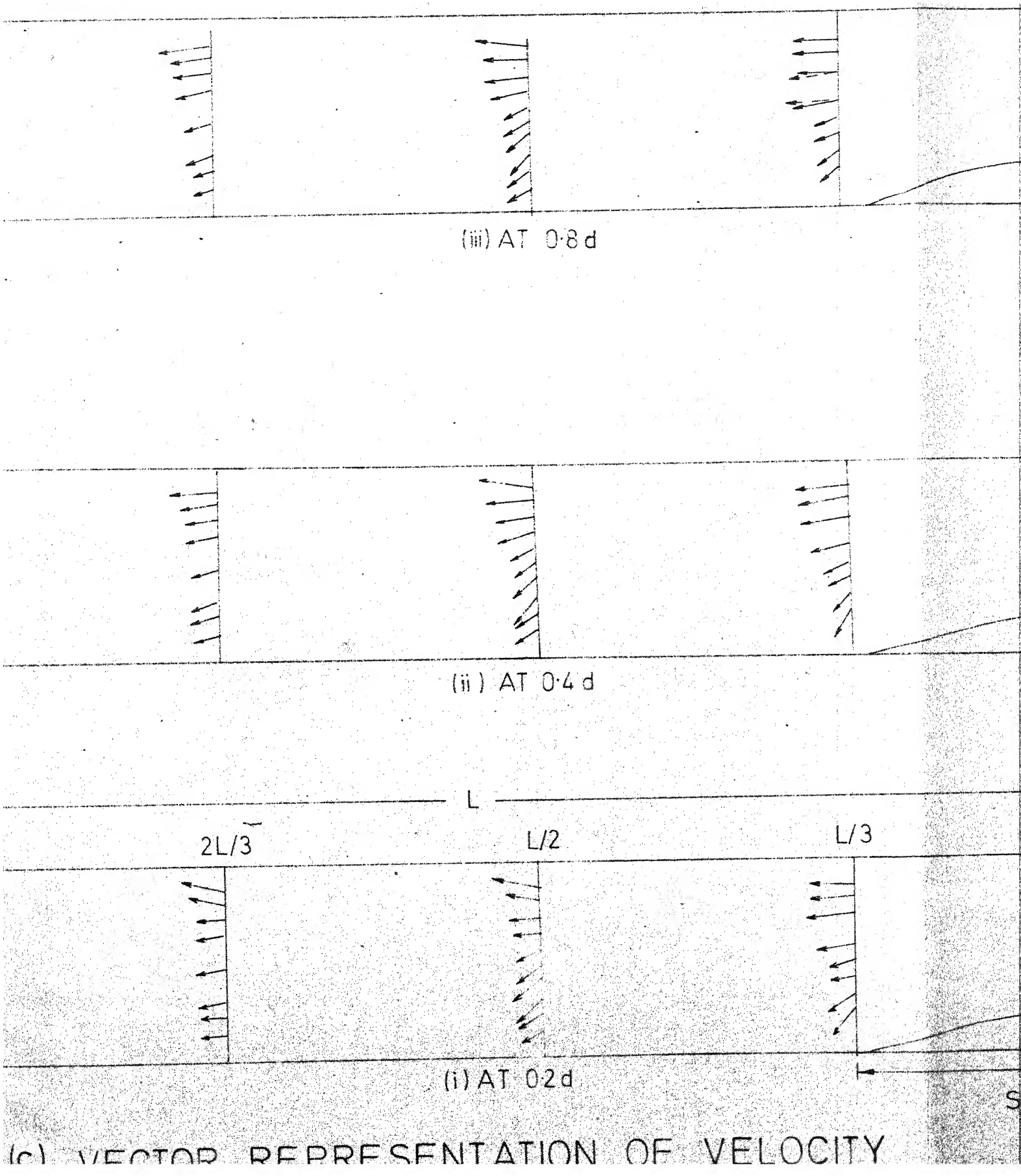

(c) VECTOR REPRESENTATION OF VELOCITY

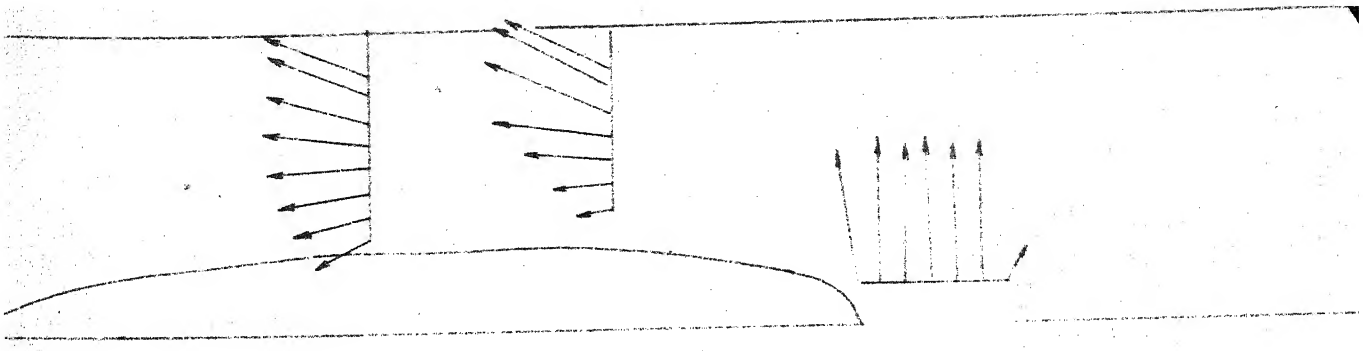

SCALE: 1 CM = 20.0 CMS/SEC

DEPTH OF FLOW 8.9 CMS (3.5 INCHES)

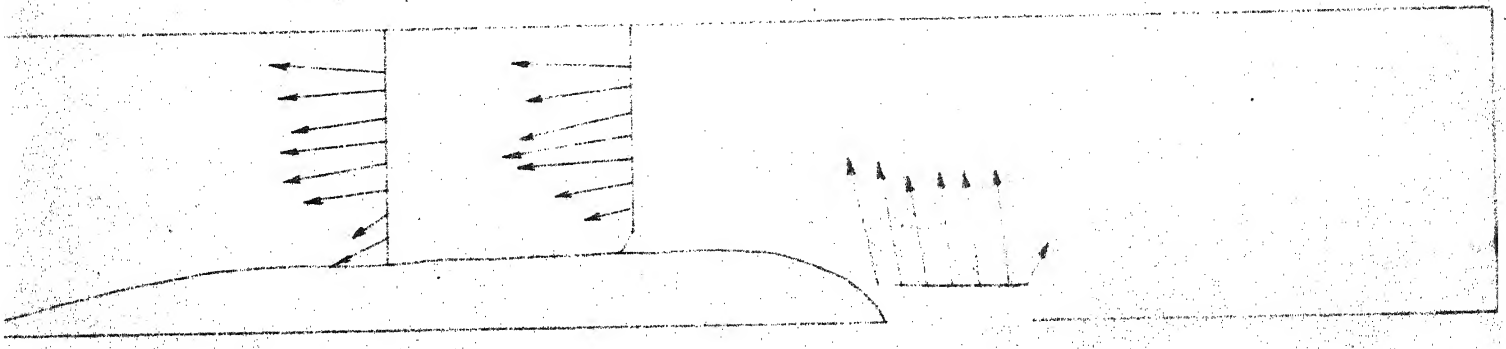

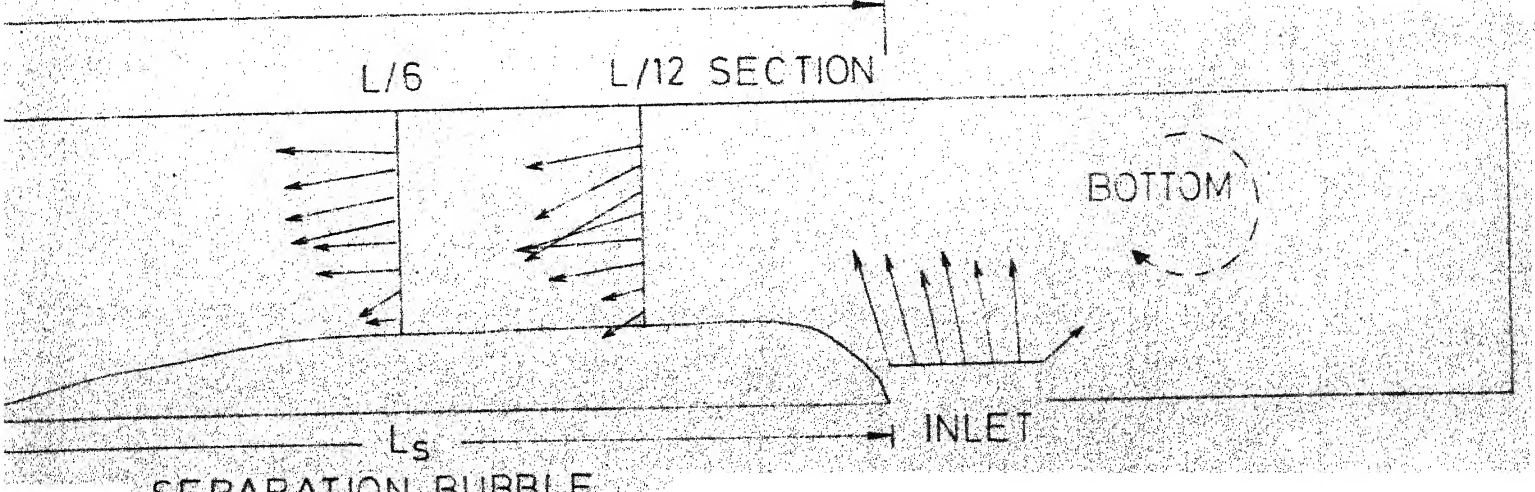

SEPARATION BUBBLE

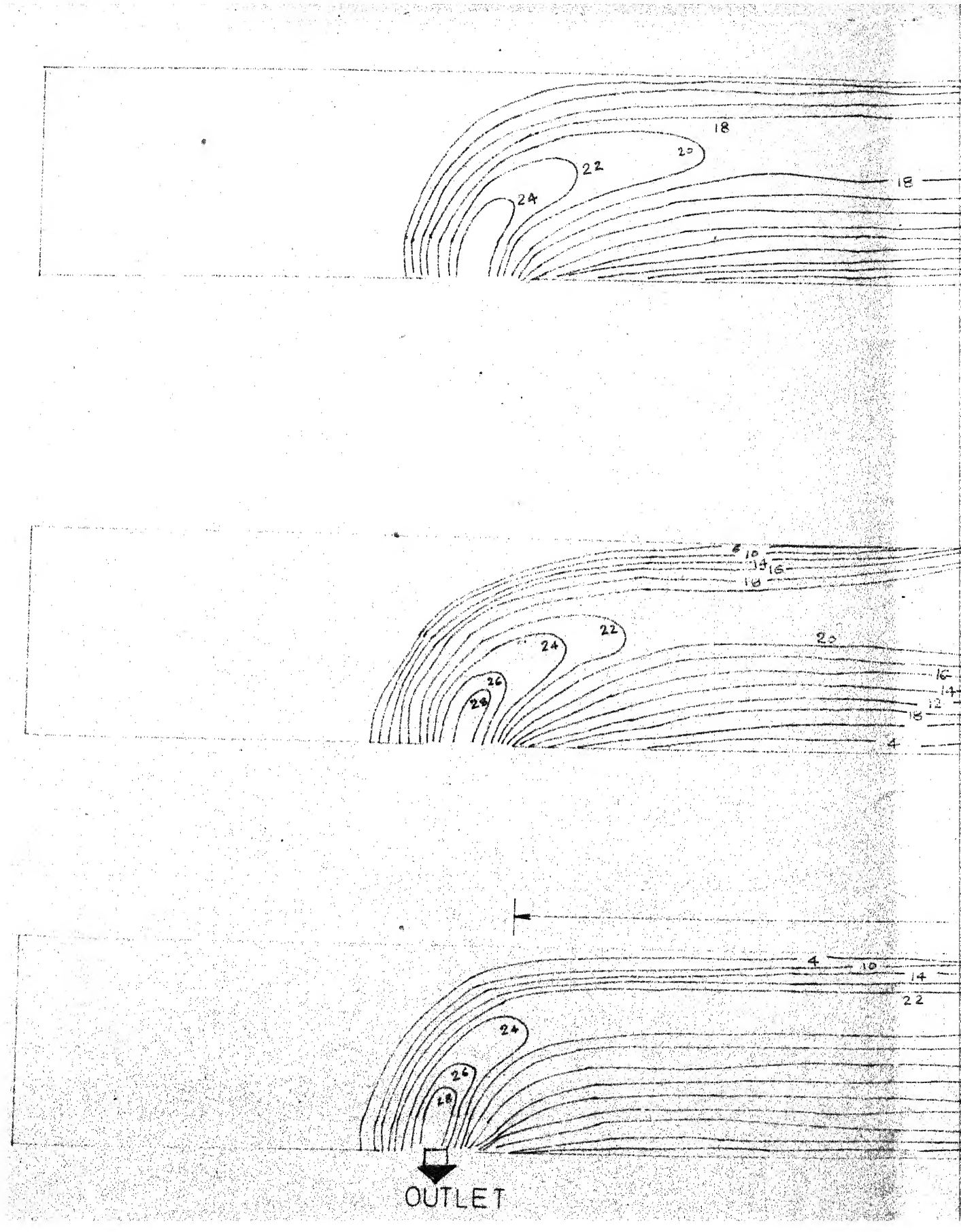
18
20
22
24
18
10
14
16
18
22
24
26
28
20
16
14
12
18
4
4
10
14
22
24
26
28
OUTLET

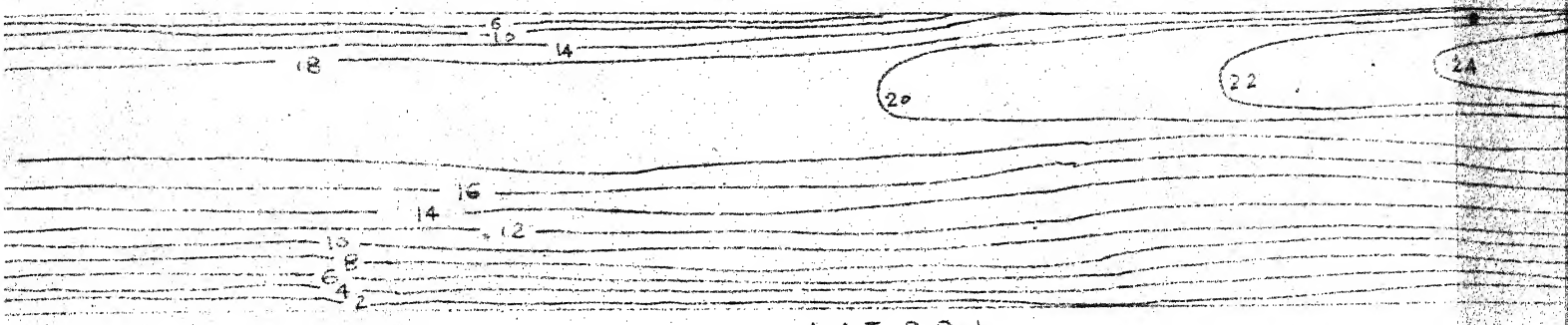

(iii) AT 0·8 d

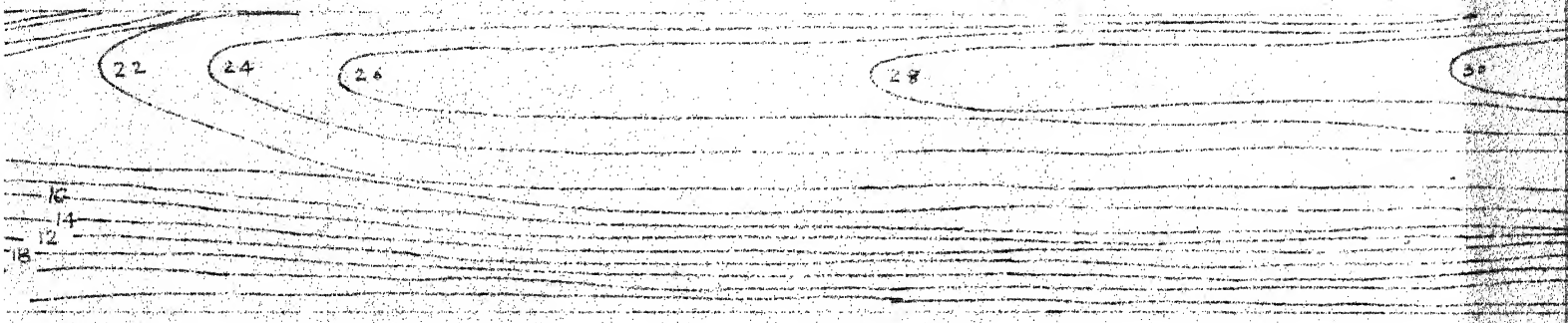

(ii) AT 0·4 d

L

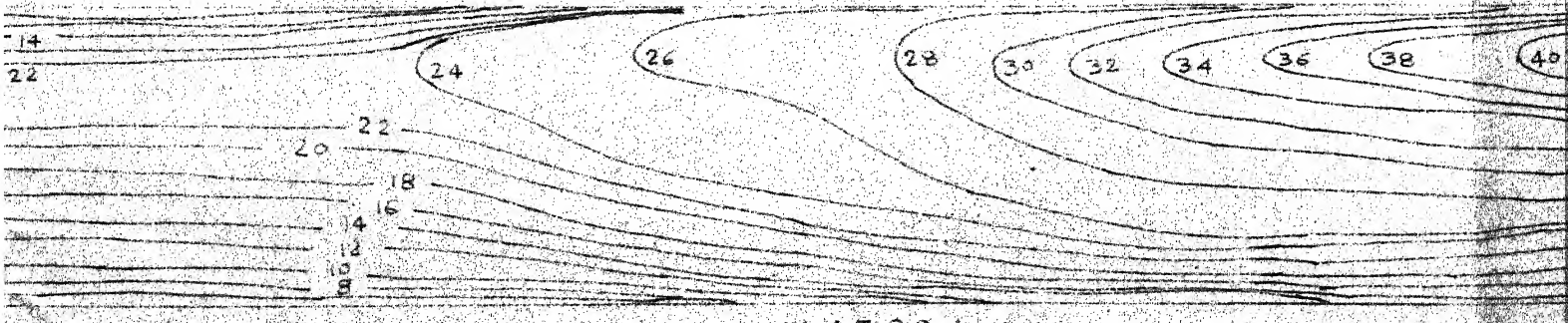

(i) AT 0·2 d

FIG 7(a) VELOCITY CONTOURS

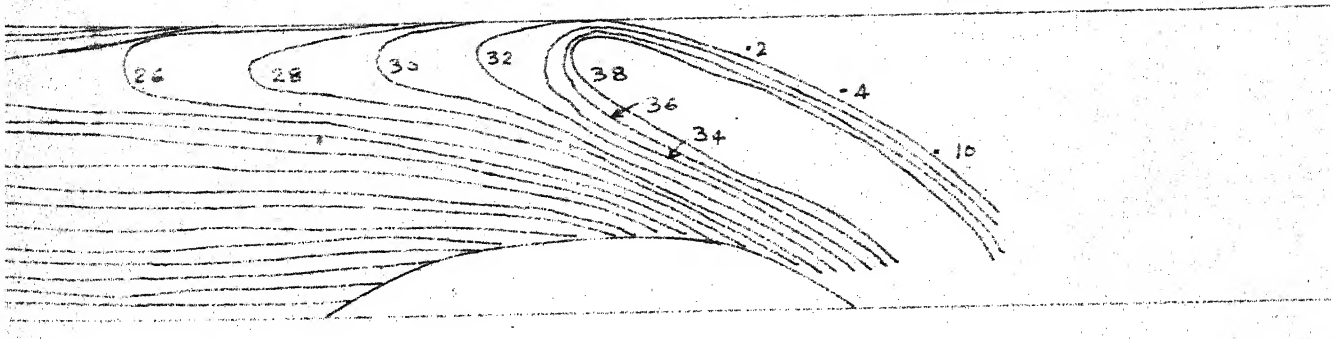

NUMBERS INDICATE VELOCITY (CM/SEC)

DEPTH OF FLOW 22·8 CMS (9 INCHES)

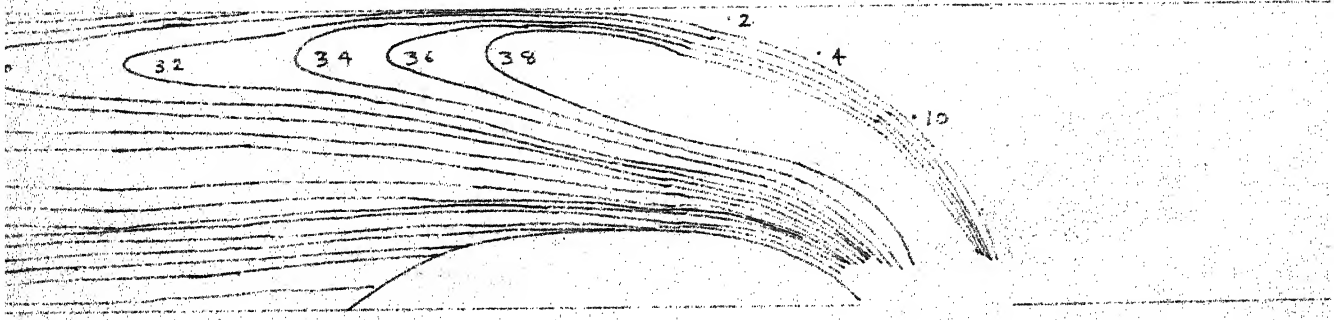

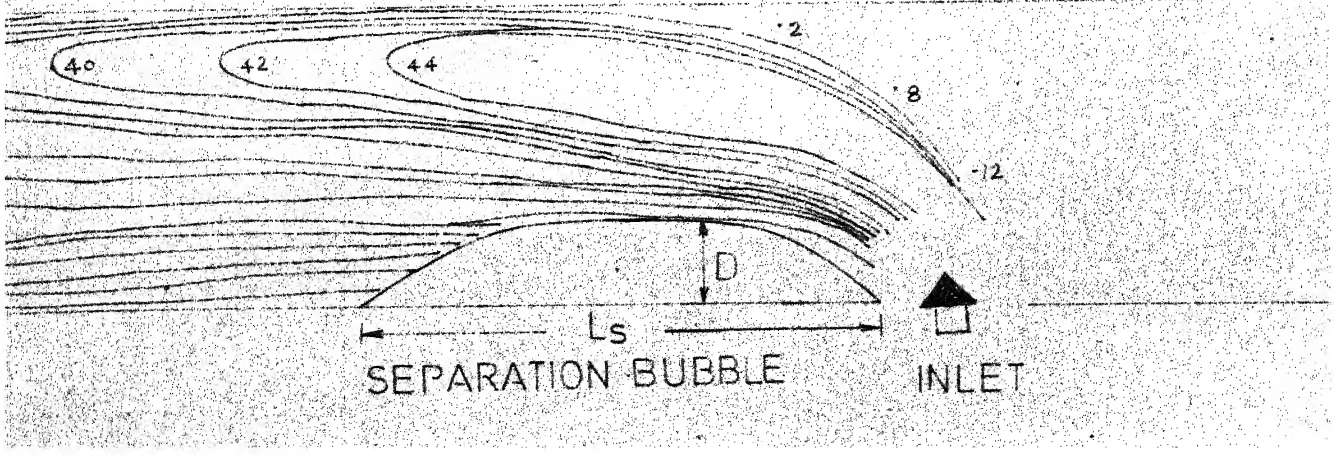

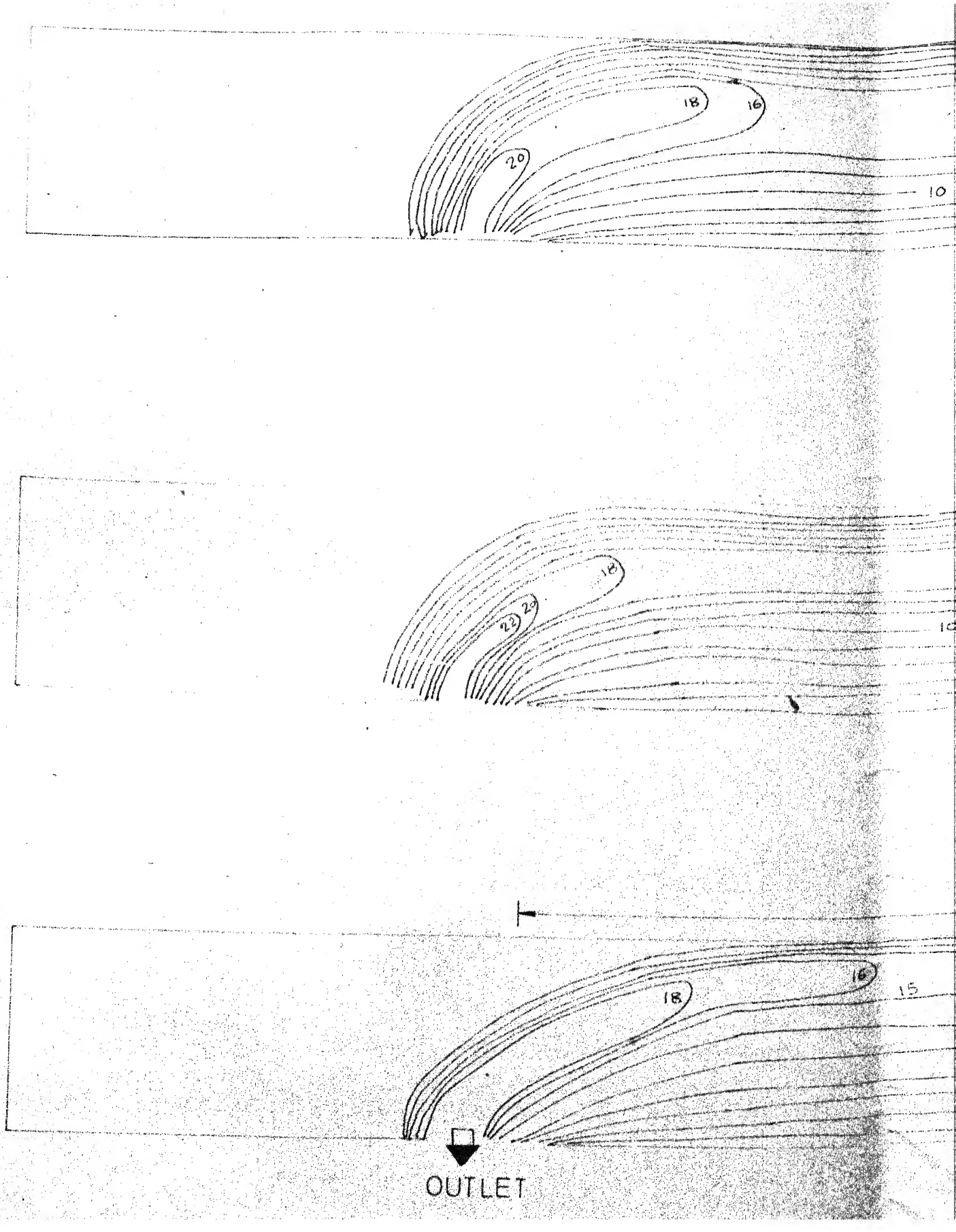
18
16
20
10
18
20
22
OUTLET

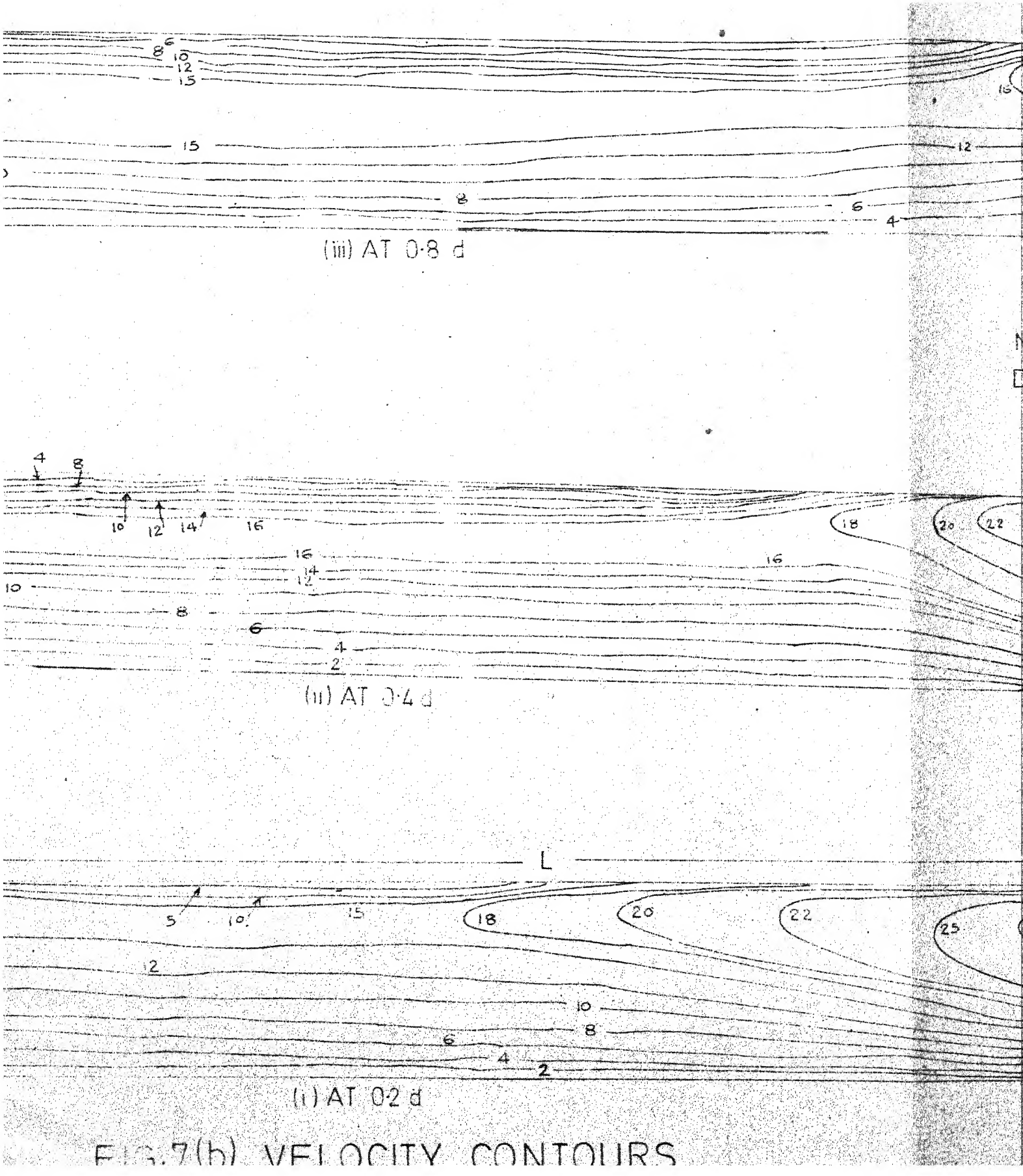

FIG.7(b) VELOCITY CONTOURS

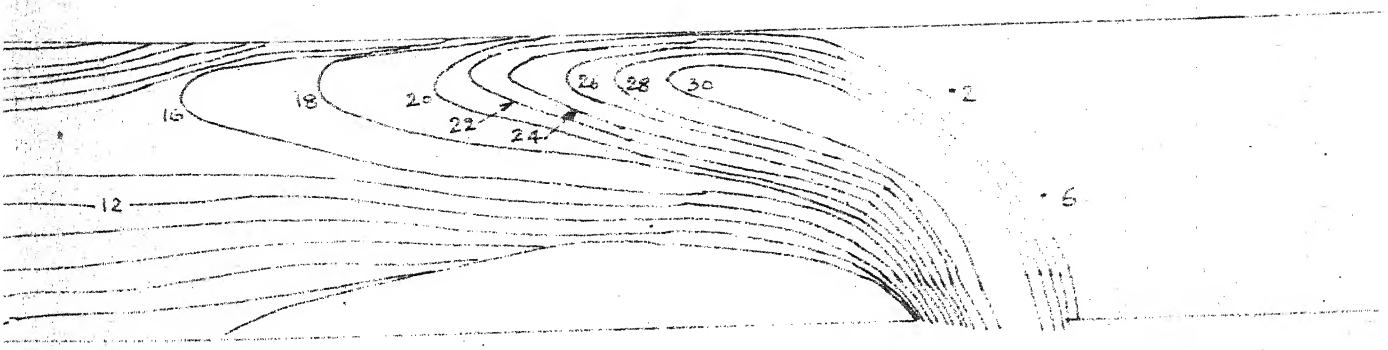

NUMBERS INDICATE VELOCITY (CM/SEC)
DEPTH OF FLOW 17.1 CMS (6.75 INCHES)

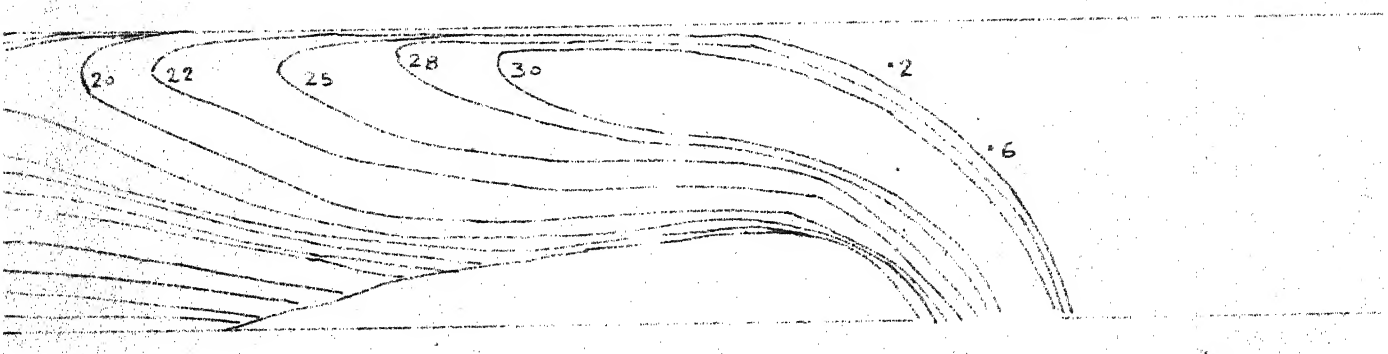

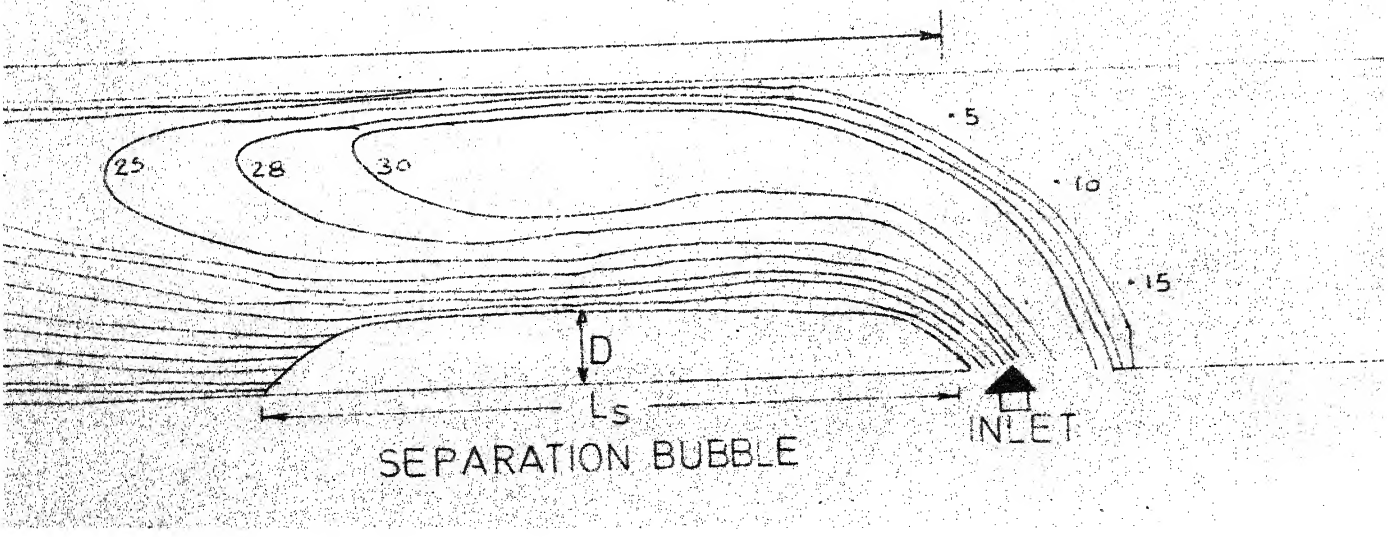

SEPARATION BUBBLE

4
6
8
12
14
16

4
10
12
14
16

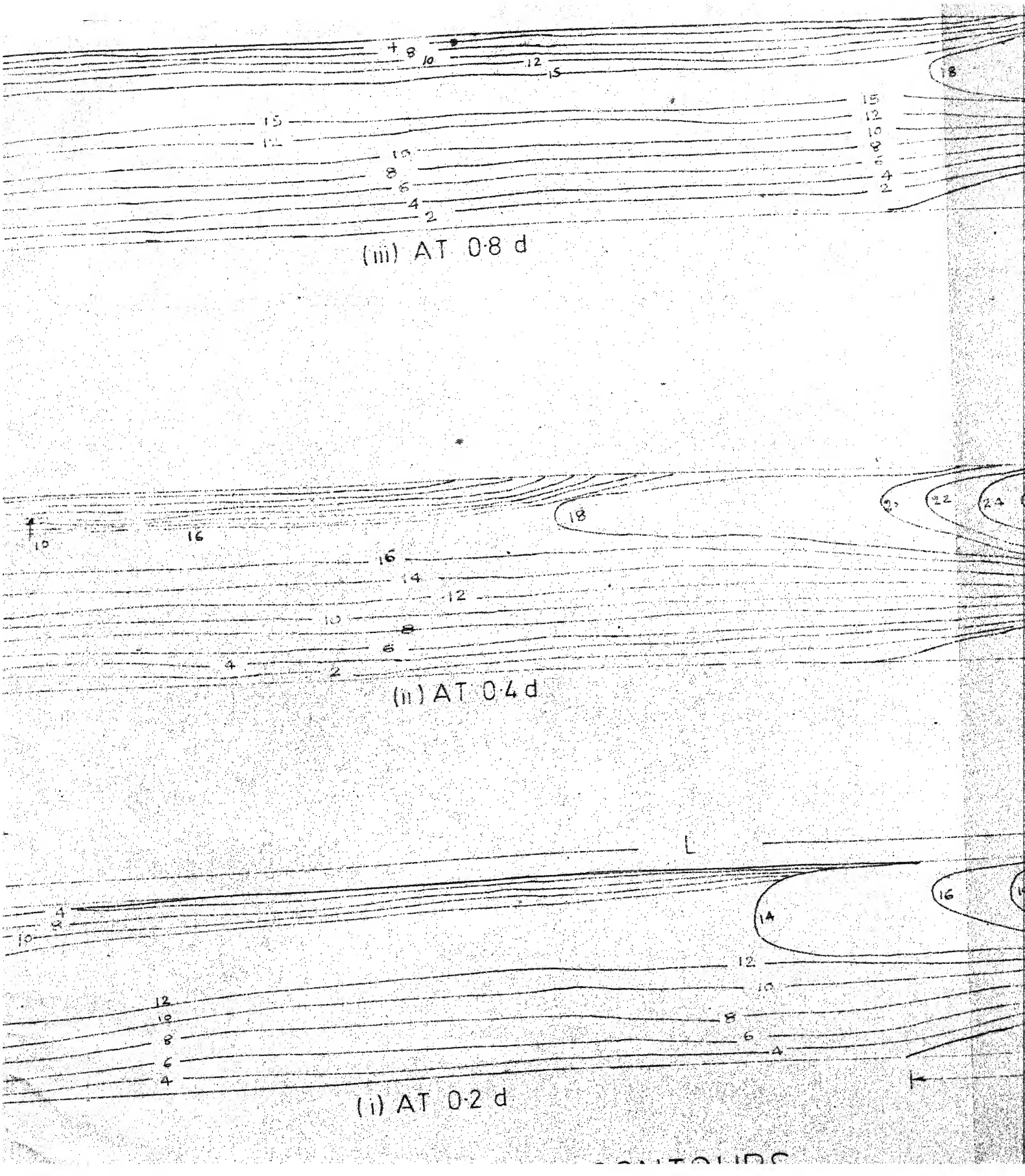
(iii) AT 0·8 d
(ii) AT 0·4 d
(i) AT 0·2 d

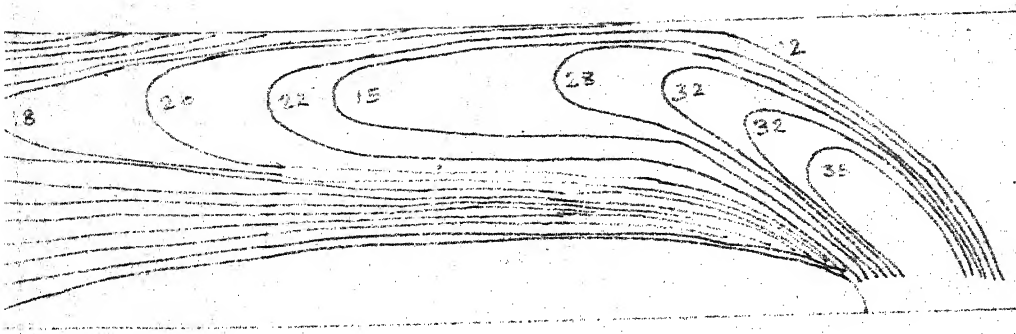

NUMBERS INDICATE VELOCITY (CMS/SEC)

DEPTH OF FLOW 8·9 CMS (3·5 INCHES)

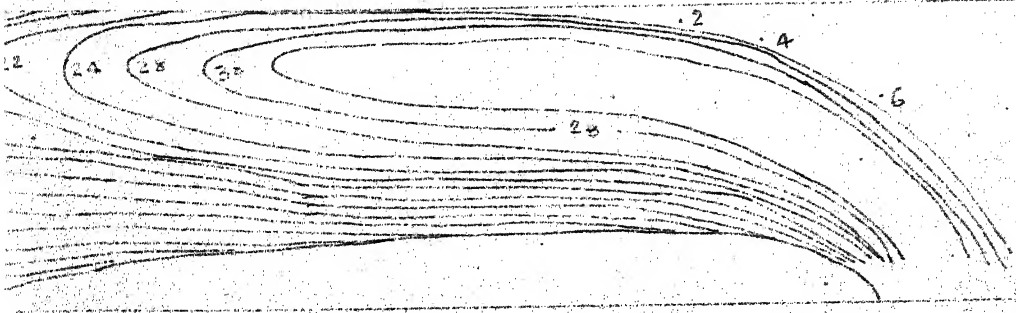

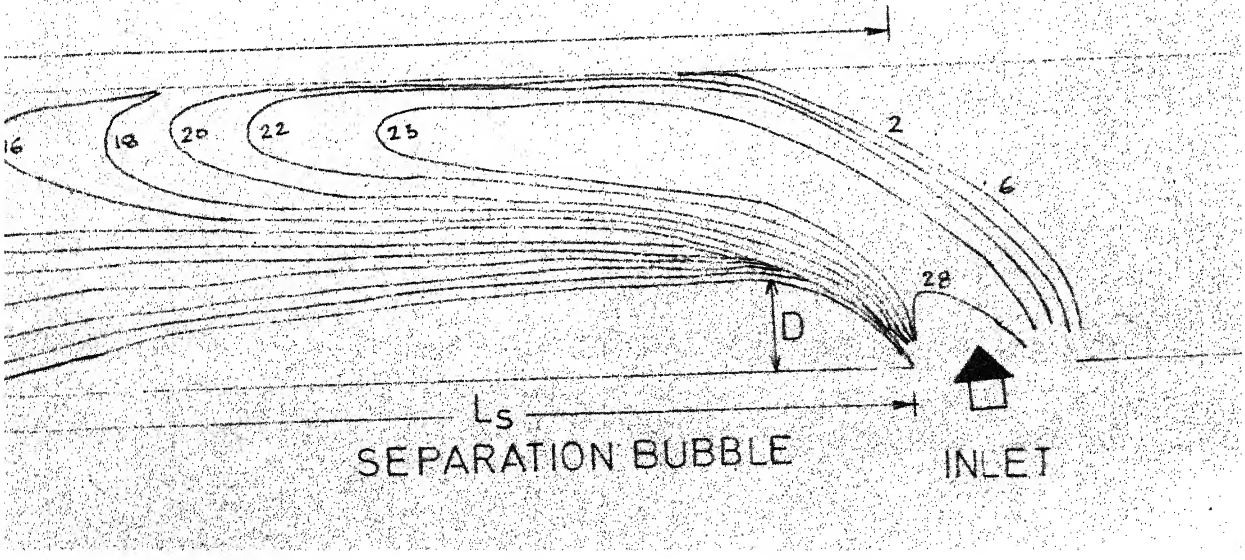

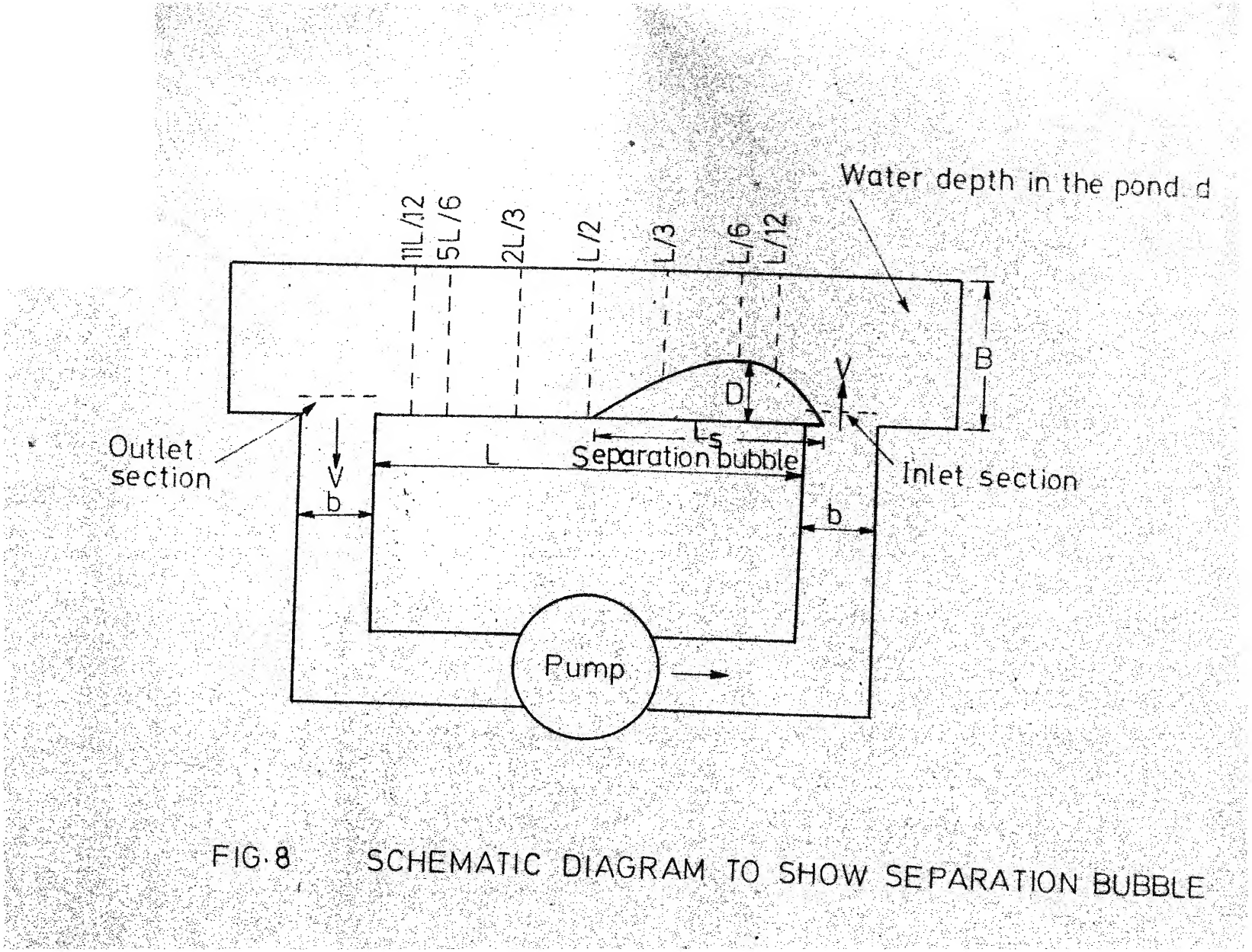

FIG·8 SCHEMATIC DIAGRAM TO SHOW SEPARATION BUBBLE

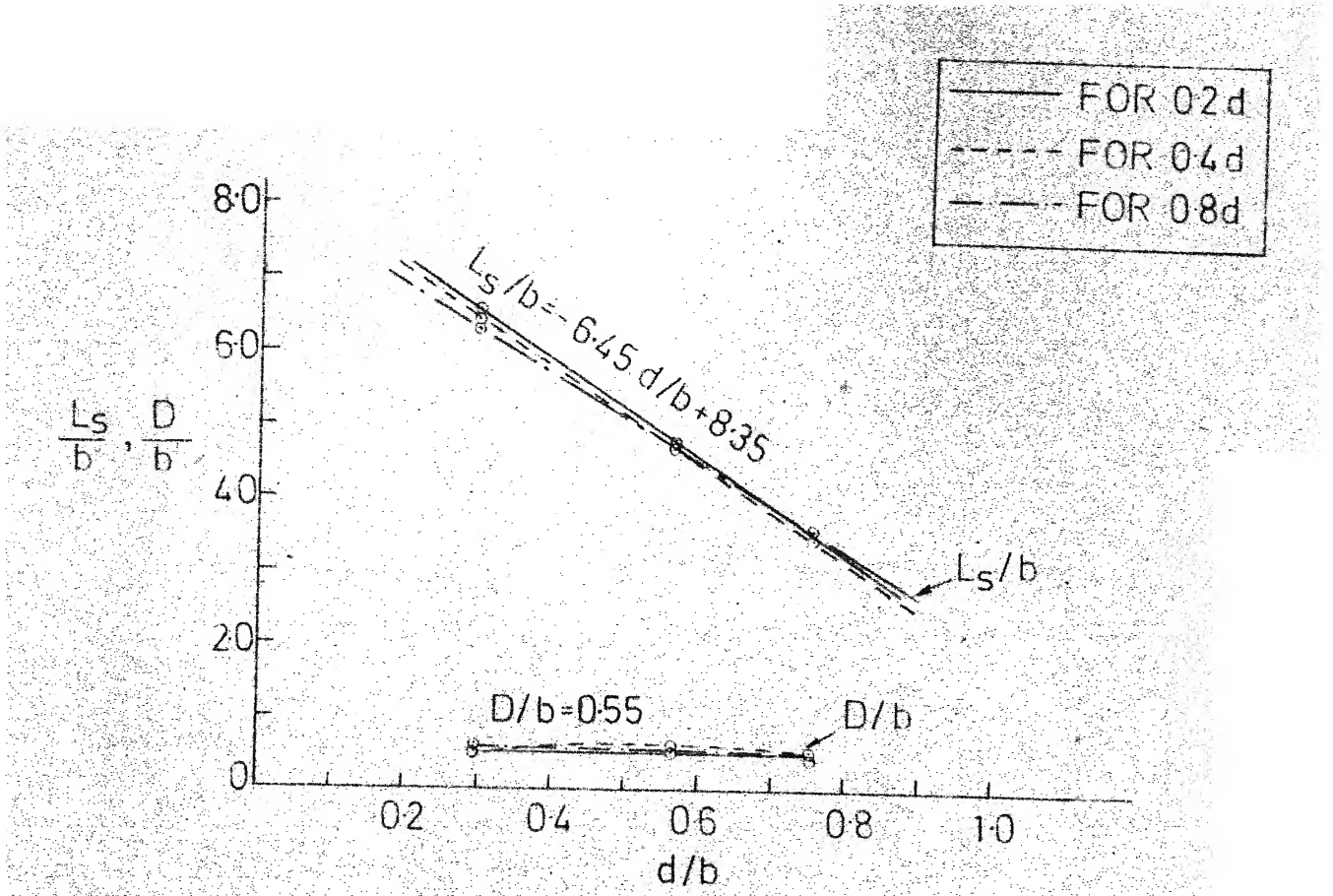

FIG. 9 GEOMETRY OF SEPARATION BUBBLE

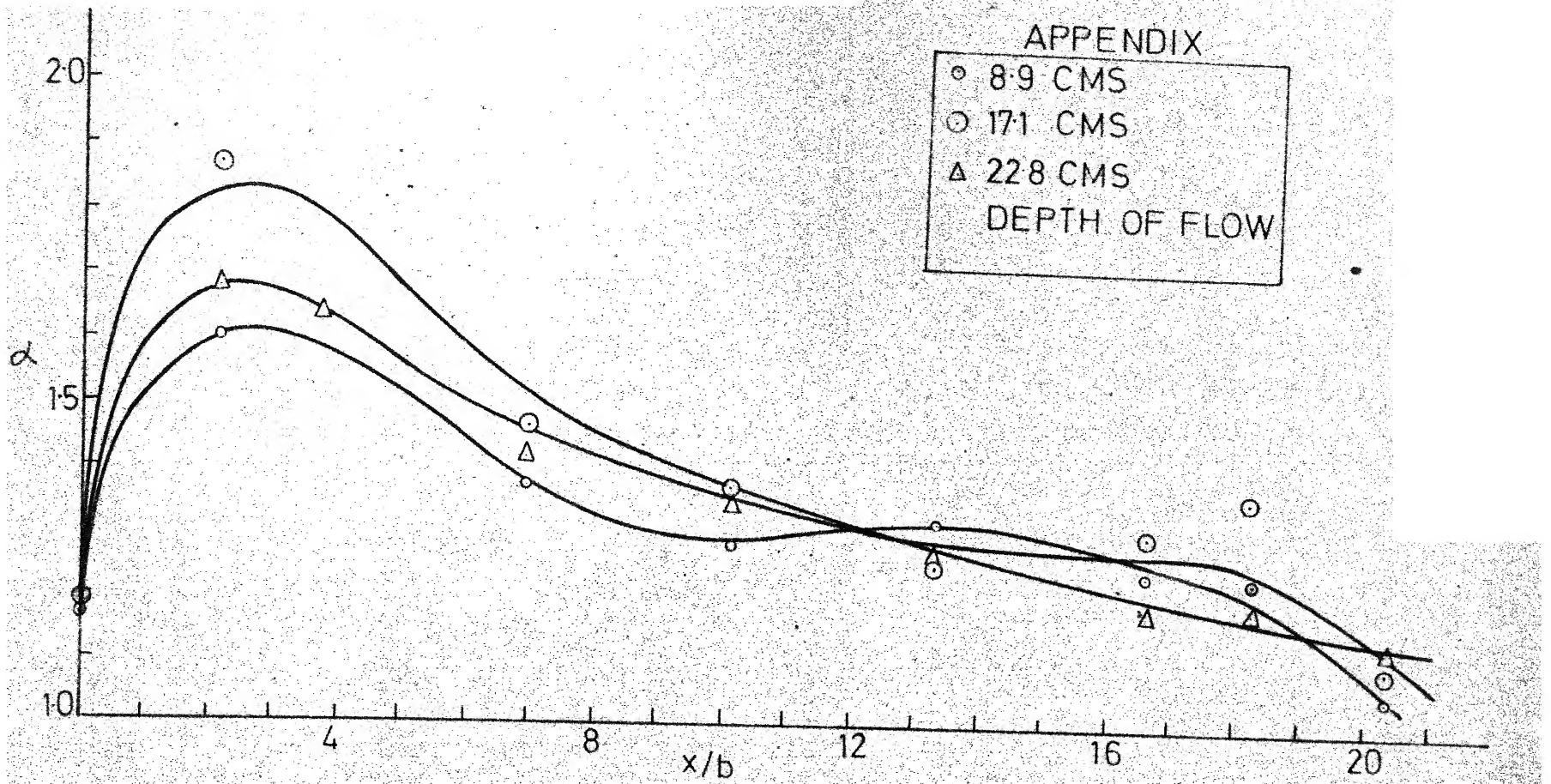

FIG·10 VARIATION OF ENERGY CORRECTION COEFFICIENT

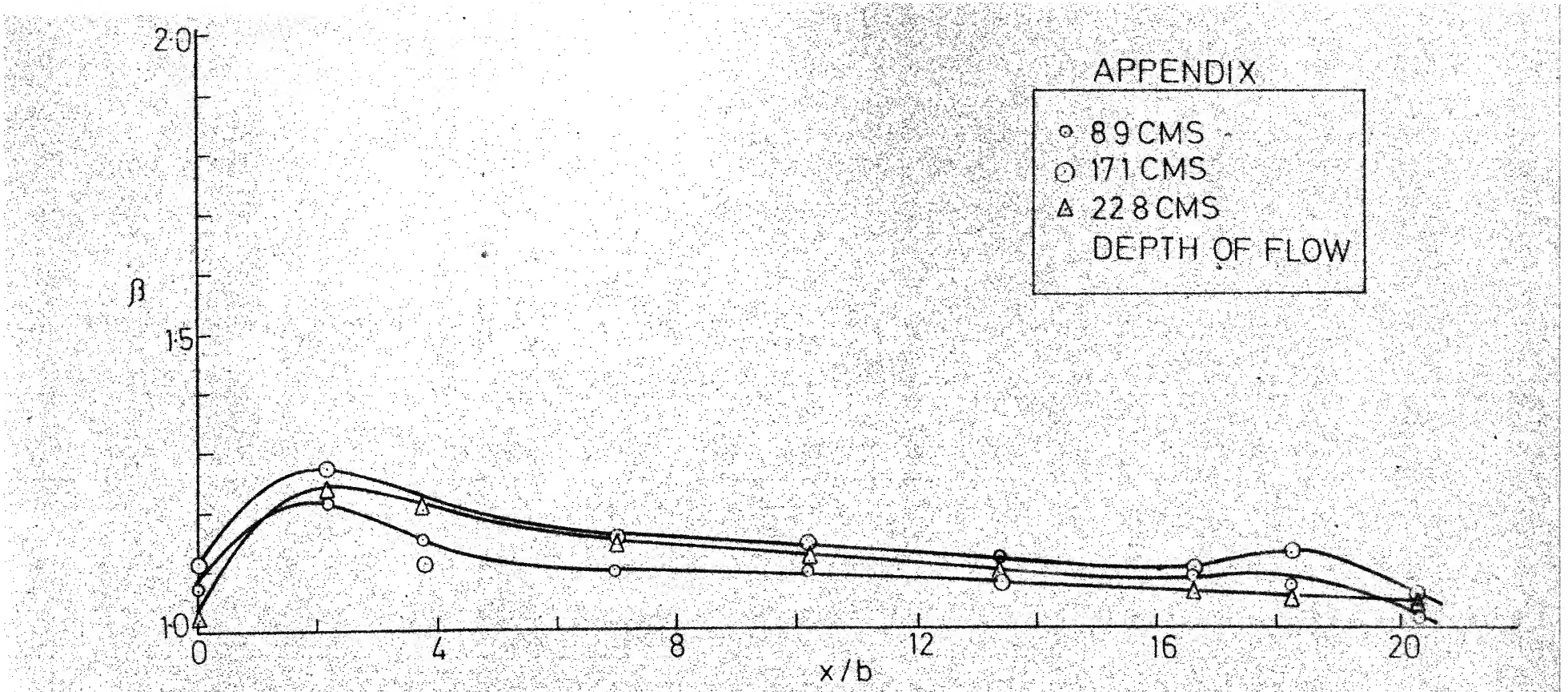

FIG-11 VARIATION OF MOMENTUM CORRECTION COEFFICIENT

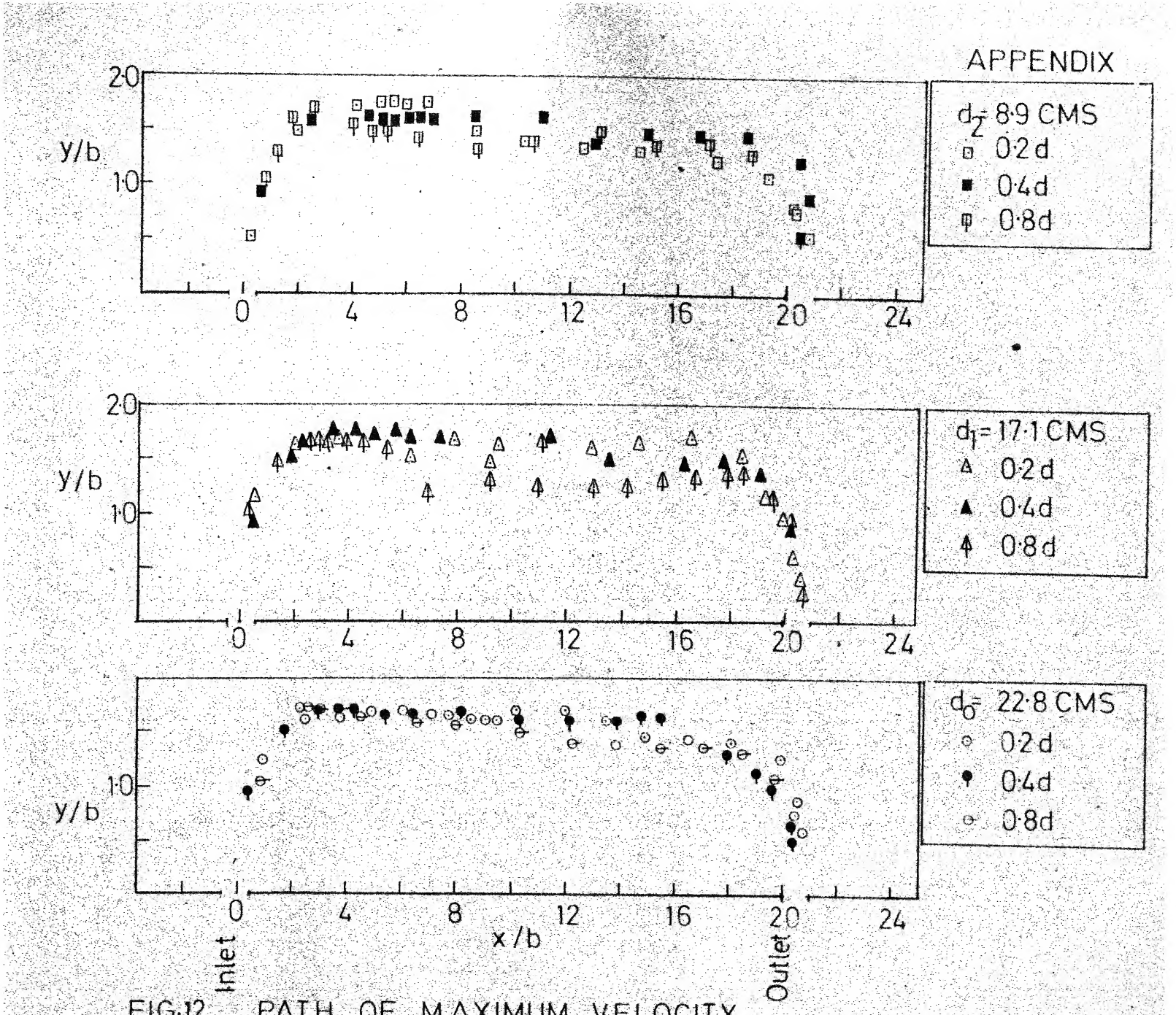

FIG·12 PATH OF MAXIMUM VELOCITY

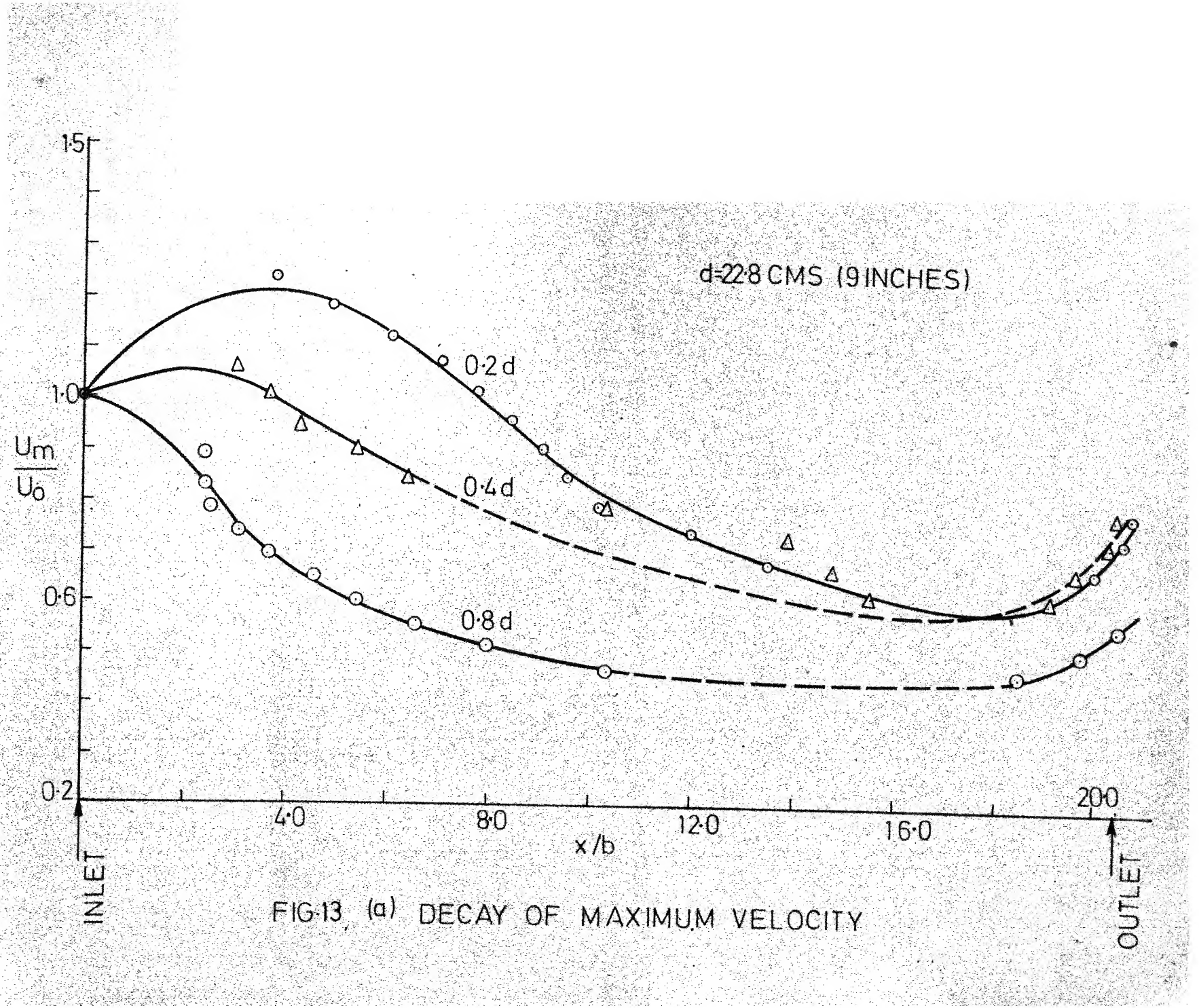

FIG·13 (a) DECAY OF MAXIMUM VELOCITY

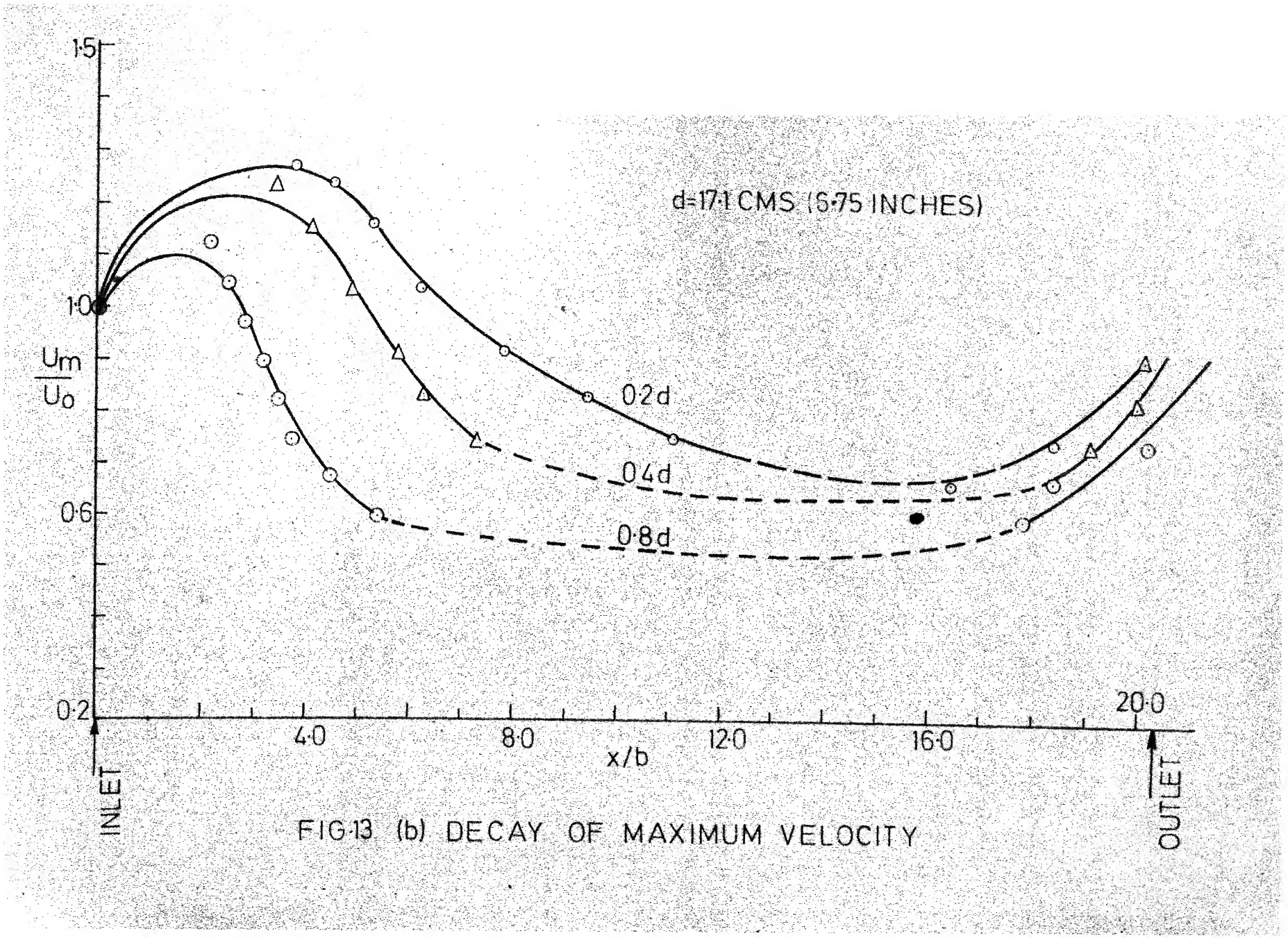

FIG·13 (b) DECAY OF MAXIMUM VELOCITY

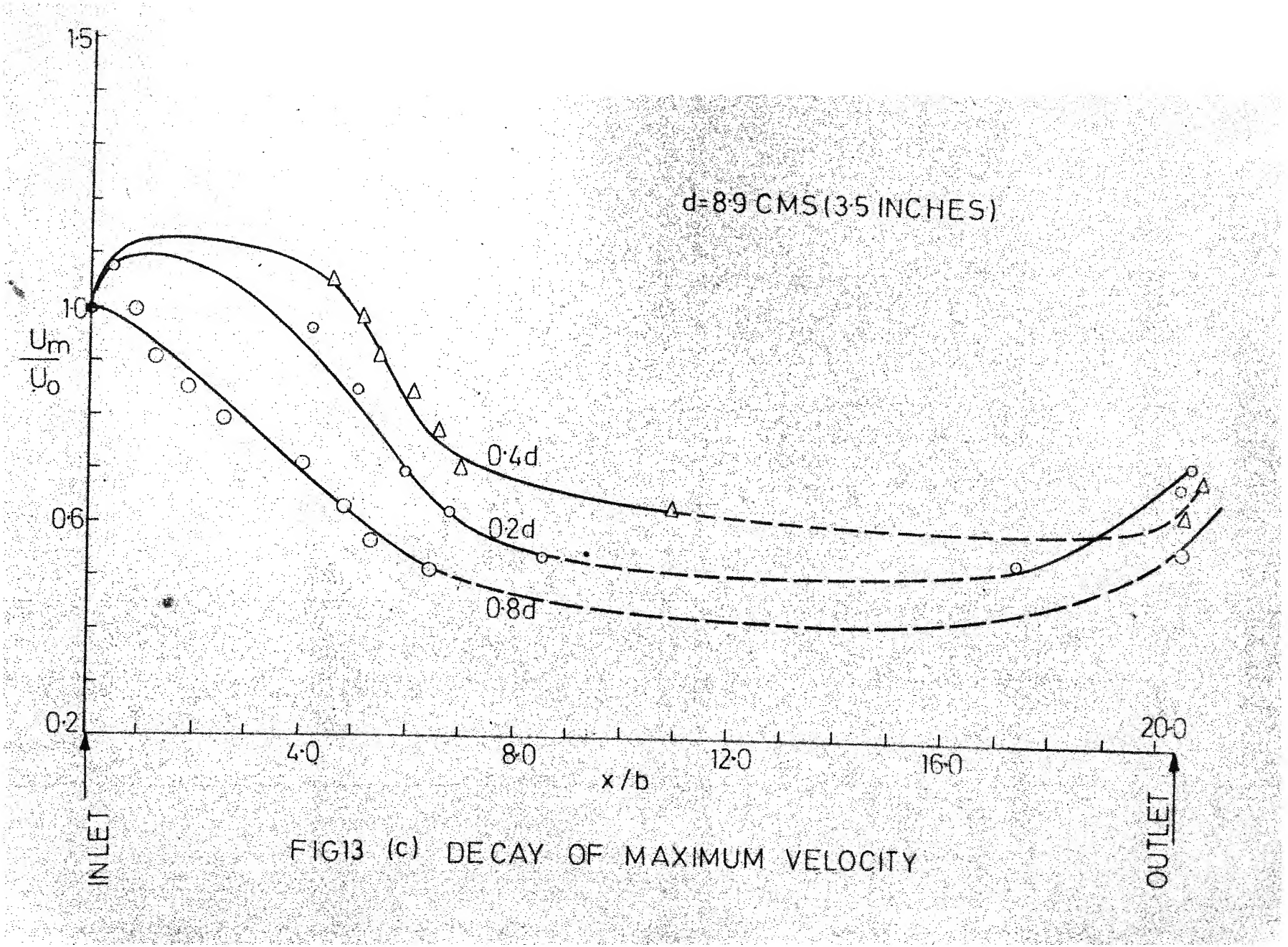

FIG13 (c) DECAY OF MAXIMUM VELOCITY

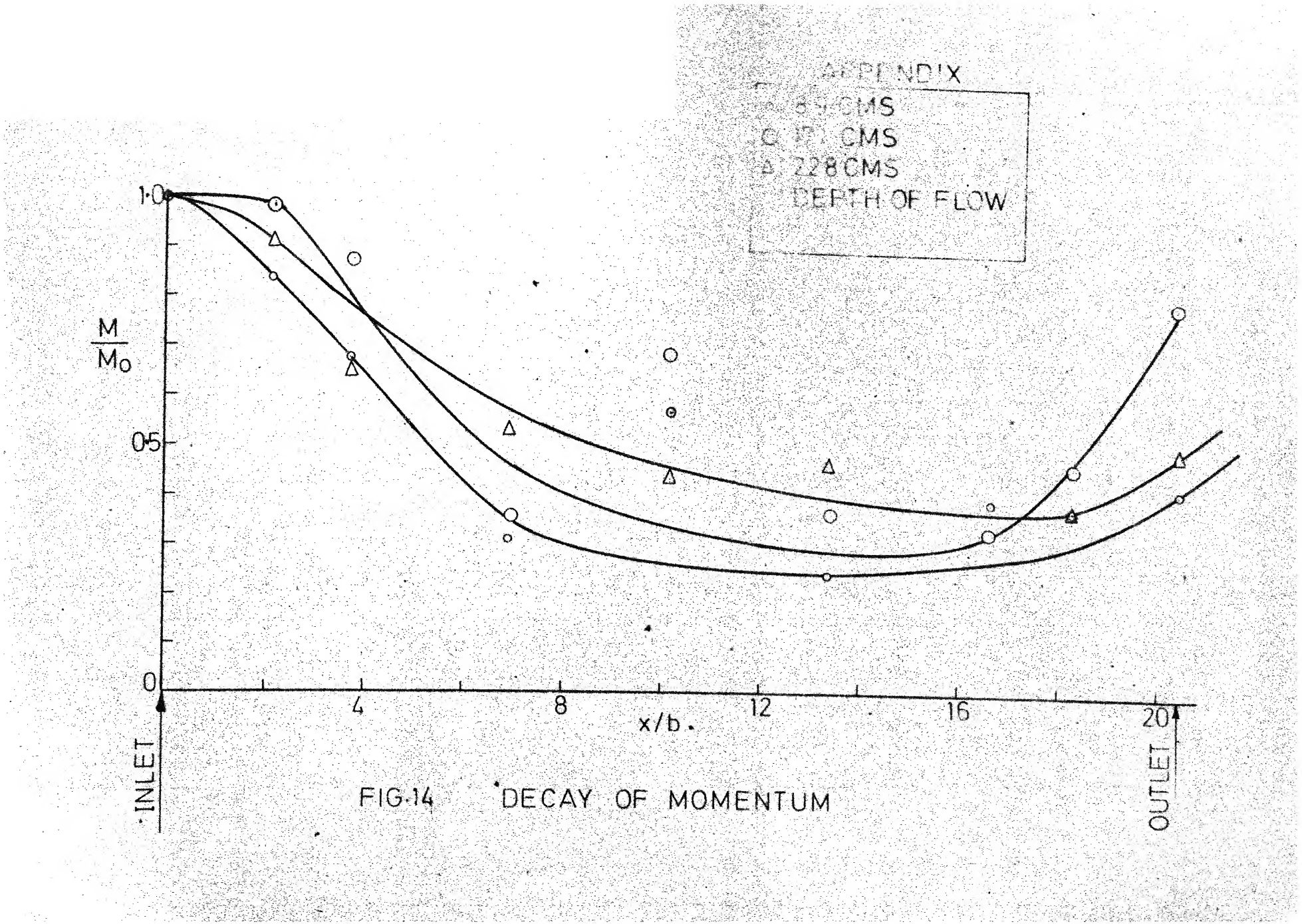

FIG-14 DECAY OF MOMENTUM

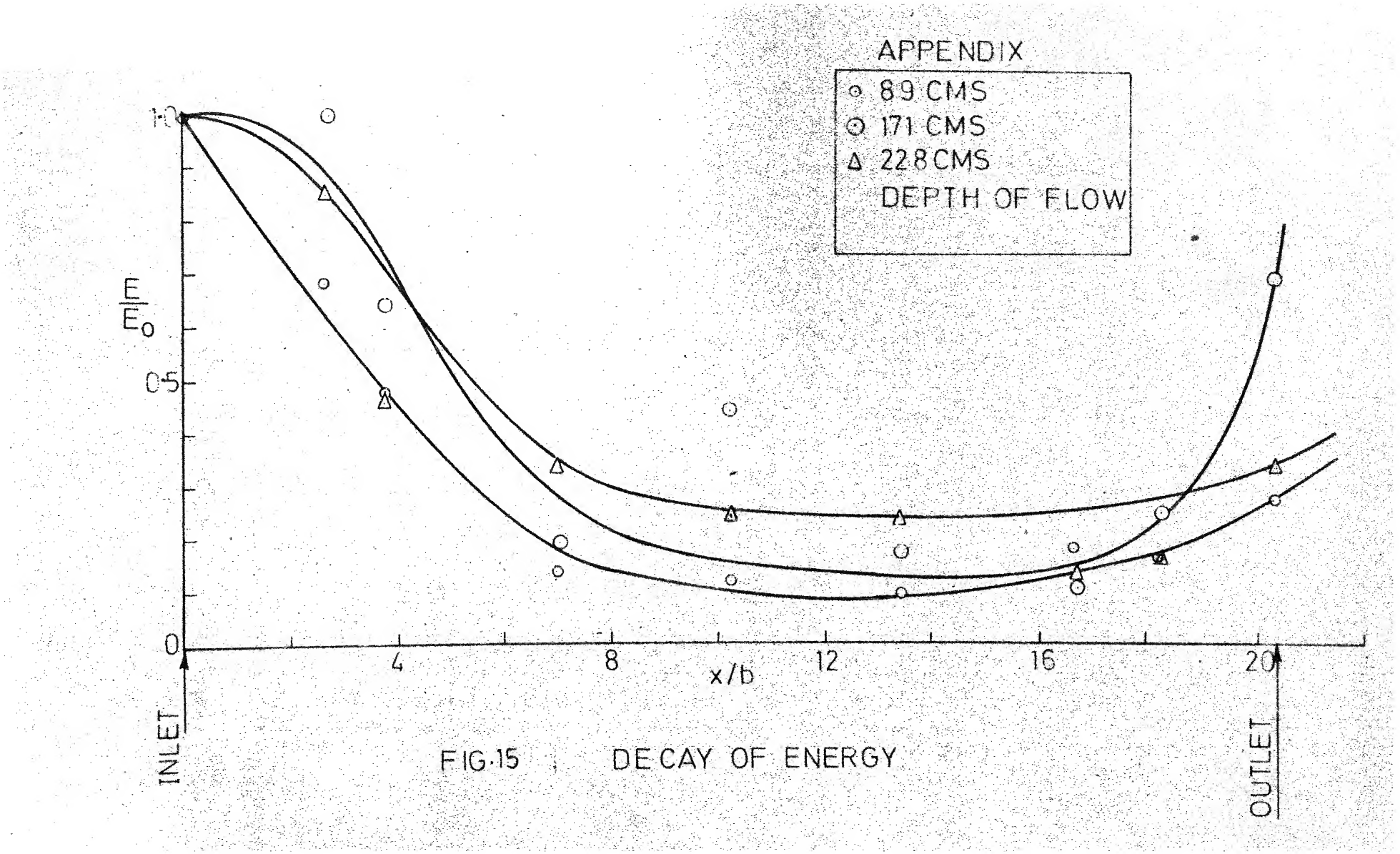

FIG·15 : DECAY OF ENERGY

BIBLIOGRAPHY

1. Sayre, W.W., 'Investigation of surface-jet Thermal Outfall for Itan Steam Electric Generating Station', Iowa Institute of Hydraulics research, The University of Iowa, IIHR Report No. 167, 1975.

2. Israngkura, Udomsak, 'Profiles of a round turbulent jet injected normally in to a cross-stream of finite depth', M.E. Thesis, Department of Civil Engg., The University of Alberta, Edmonton, 1972.

3. Chow, V.T., 'Open Channel Hydraulics', McGraw-Hill Book Company, Inc.

4. Rajaratnam, N., and Subramanya, K., 'The diffusion of rectangular wall jets in wide channels', Journal of Hydraulic Research, International Association of Hydraulics Research, Vol. 5, 1967.

5. Boericke, R.R., and Hall, D.W., 'Hydraulics and Thermal dispersion in an irregular estuary', Journal of Hydraulics Division, ASCE, Vol. 100, N. HY1, January 1974.

6. Paily, P.P., et. al., 'Winter-Regime thermal response of heated-streams', Journal of Hydraulics Division, ASCE, Vol. 100, No. HY4, April, 1974.

7. Shirazi, M.A., et.al., 'Heated water jet in co-flowing turbulent-stream', Journal of Hydraulics Division, ASCE, Vol. 100, No. HY7, July 1974.

8. Weil, James, and Fisher, H.B., 'Effect of Stream turbulence on heater water plumes', Journal of Hydraulics Division, ASCE, Vol. 100, HY.7, July, 1974.

9. Townsend, R.D., and Egar, D.L., 'Rapid Temperature Reduction of Thermal Discharge', Journal of Hydraulics Division, ASCE, Vol. 101, No. HY 5, May, 1975.

10. List, E.J., and Imberger, J., 'Turbulent Entrainment in Buoyant jets and plumes', Journal of Hydraulics Division, ASCE, Vol. 99, No. HY 9, Sept. 1973.

11. Richardson, E.V. and Miller, A.C., 'Diffusion and Dispersion in open channel Flow', Journal of Hydraulics Division, ASCE, Vol. 100, No. HY1, Jan.1974.

12. Peterson, J.P., et.al. 'Enhanced Dispersion in Drag Reducing Open Channel Flow', Journal of Hydraulics Division, ASCE, Vol. 100, No. HY 6, June, 1974.

13. Narain, J.P., 'Swirling Shallow Submerged Turbulent Plumes', Journal of Hydraulics Division, ASCE, Vol.100, No. HY 9., Sept. 1974.

14. Cederwall, K., 'Gross Parameter Solutions of Jets and Plumes', Journal of Hydraulics Division, ASCE, Vol. 101, No. HY5, May, 1975.

15. Atesman, K.M., 'Point Source Dispersion in Turbulent Open Channels', Journal of Hydraulics Division, ASCE, Vol. 101, No. HY 7, July, 1975.

APPENDIX A1

d = 22.8 cm and F = 0.215

θ = direction of flow in degrees as shown in Fig. 6(a,b,c)

Section Inlet (9 cm. away from wall	Distance in cm from inlet in U/S and D/S direction	0.2d V in cm/sec.	0.2d θ in degrees	0.4d V in cm/sec.	0.4d θ in degrees	0.8d V in cm/sec.	0.8d θ in degrees
1	2	3	4	5	6	7	8
''	-15.0	21.0	83.5	22.0	83.5	41.0	81
''	-10.0	36.0	78.5	34.6	81.0	43.0	83
''	- 5.0	33.5	81.0	34.6	79.0	38.0	79
''	0.0	35.0	79.0	36.4	79.0	41.5	79
''	5.0	40.0	78.0	40.0	77.8	48.5	81
''	10.0	43.0	76.0	43.0	77.5	50.2	79
''	15.0	40.0	71.0	40.0	71.0	41.5	77
L/12	From inner wall towards outer wall	V	θ	V	θ	V	θ
''	54.0	45.0	2.5	46.0	13.0	46.8	16.0
''	50.0	46.0	0	46.0	21.0	46.8	17.0
''	45.0	40.0	350	46.8	22.0	42.5	16.5
''	40.0	44.0	345	40.0	11.0	36.4	14.0

Contd.

Contd. Appendix A1

1	2	3	4	5	6	7	8
L/12	from inner wall towards outer wall	V	θ	V	θ	V	θ
''	35.0	39.0	353	32.0	3.5	33.0	6
''	30.0	33.0	353	25.5	359	21.0	12
''	25.0	18.3	356	15.3	14	4.0	21
''	20.0	11.0	355	9.8	356	0.0	0
L/6	Distance from inner wall towards outer wall.	V	θ	V	θ	V	θ
''	54.0	42.5	0	41.0	6	40.0	10
''	50.0	42.5	357	37.0	4	35.0	10
''	45.0	36.4	353	31.5	5	28.5	9
''	40.0	35.0	346	28.5	0	23.5	13
''	35.0	27.5	341	25.5	355	22.0	4
''	30.0	32.0	334.5	21.0	348	17.0	6
''	25.0	28.5	334.5	23.5	341	11.0	341
''	20.0	24.6	323	15.3	326	11.0	326
''	17.0	23.5	318.5	23.5	323	11.0	313
''	15.0	20.0	315.5	11.0	304.5	11.0	291
''	9.0	7.5	280	13.8	280	0	0

Contd.

Contd. Appendix A1

1	2	3	4	5	6	7	8
/ L/3	Distance in cm from inner wall towards outer wall	V	θ	V	θ	V	θ
''	54.0	36.4	4.0	33.5	6.5	30.5	15
''	50.0	37.0	357.5	30.0	2.5	24.6	14
''	45.0	34.6	353	25.5	2.0	21.0	12
''	40.0	33.5	350.5	25.5	353	15.3	17
''	35.0	32.0	349	21.0	353	17.0	17
''	30.0	31.5	344	18.3	1	17.0	17.5
''	25.0	27.5	346.5	23.5	351	17.0	13.5
''	20.0	23.5	346.0	18.3	346	18.3	8.5
''	15.0	21.0	340.0	21.0	346.5	11.0	7
''	9.0	17.0	351	11.0	358	11.0	23
L/2	54.0	29.0	358.5	24.6	6	23.5	19
''	50.0	28.5	358.5	25.5	0	22.0	15
''	45.0	29.0	358.0	25.5	358	20.0	12.5
''	40.0	27.5	356.5	27.5	356.5	21.0	11.0
''	35.0	25.5	356	23.5	356	18.3	10.0
''	30.0	25.5	356	23.5	356	18.3	10.0

Contd.

1	2	3	4	5	6	7	8
L/2	From inner wall towards outer wall	V	θ	V	θ	V	θ
''	20.0	20.0	353.5	17.0	355	15.3	10
''	15.0	20.0	347.5	15.3	355	13.8	7
''	9.0	15.3	354.0	13.8	357	11.0	5
2L/3	54.0	23.5	3.5	24.6	3.5	29.0	3.5
''	50.0	23.5	1.0	27.5	4.0	24.6	10
''	45.0	27.5	0.0	25.5	5.0	23.5	8
''	35.0	21.0	357.5	23.5	357	21.0	5.5
''	25.0	21.0	354.0	21.0	354	18.3	1.0
''	20.0	18.3	350	18.3	350.5	17.0	5.5
''	15.0	20.0	350	17.0	350	17.0	355
''	9.0	17.0	350	17.0	351	17.0	354
5L/6	54.0	17.0	359.5	21.0	1	18.3	9.5
''	50.0	20.0	356.0	20.0	356	21.0	356
''	45.0	18.3	356.0	18.3	356	23.5	356
''	35.0	15.3	356.0	15.3	356	15.3	1
''	25.0	17.0	353	15.3	356	17.0	356

Contd.

Contd. Appendix A1

1	2	3	4	5	6	7	8
5L/6	From inner wall towards outer wall	V	θ	V	θ	V	θ
''	17.0	15.3	353	17.0	353	17.0	353
''	13.0	18.3	2.5	20.0	358.5	21.0	358.5
''	9.0	18.3	0	18.3	0	18.3	0
11L/12	54.0	17.0	357	17.0	359.5	18.3	3
''	50.0	17.0	354	17.0	355	17.0	1
''	40.0	20.0	354	18.3	358	18.3	1.5
''	30.0	18.3	353.5	20.0	355	20.0	355
''	20.0	20.0	356.5	20.0	356.5	20.0	359
''	14.0	20.0	356.5	20.0	355.0	21.0	355
''	9.0	20.0	0	21.0	358.5	21.0	358.5
Outlet (9cm away from wall)	-15.0	26.5	324.5	27.5	33	30.5	334
''	-10.0	29.0	312.5	29.0	319	30.5	324
''	- 5.0	28.0	298.5	29.0	308	29.5	315
''	0	33.0	280.0	32.0	301	29.0	311
''	5.0	30.5	281	29.0	294.5	28.5	302
''	10.0	25.5	257	26.5	283.5	26.5	294
''	15.0	18.3	249	18.3	276	15.3	298

APPENDIX A2

d = 17.1 cm and F = 0.215

θ = Direction of flow in degrees as shown in Fig. 6 (a,b,c).

		0.2d		0.4d		0.4d	
Section Inlet (9 cm away from wall)	Distance in cm from inlet in U/S and D/S direction	V in cm/ Sec.	θ in degrees	V in cm/ Sec.	θ in degrees	V in cm./ sec.	θ in degrees
1	2	3	4	5	6	7	8
''	-15.0	18.0	98	15.3	90	20.0	89
''	-10.0	25.5	83.	26.5	87	30.5	90
''	- 5.0	21.0	72	23.5	77	25.5	85
''	0	24.6	69	25.5	81	30.5	86
''	5.0	27.5	73	27.5	78	32.0	85
''	10.0	32.0	72	33.5	75	35.0	82
''	15.0	21.0	64	18.3	61	13.8	59
L/12	from inner wall towards outer wall	V	θ	V	θ	V	θ
''	54.0	30.5	350	30.5	10	35.0	21
''	49.0	31.5	337	33.5	15	33.5	24
''	44.0	33.0	334	32.0	1	30.5	17

Contd.

1	2	3	4	5	6	7	8
L/12	From inner wall towards outer wall	V	θ	V	θ	V	θ
''	39.0	32.0	354	30.0	0	22.0	22
''	34.0	28.5	355	20.0	2	13.8	21
''	29.0	15.3	3	13.8	3	7.5	47
''	24.0	7.5	45	7.5	5	11.0	43
''	19.0	0	0	0	0	9.8	41
L/6	54.0	23.5	1	24.6	1	23.5	10
''	49.0	33.0	356	29.0	5	23.5	22
''	44.0	30.0	346	25.5	357	21.0	19
''	39.0	30.0	342	28.5	348	18.3	12
''	34.0	29.0	350	27.5	358	18.3	12
''	29.0	24.6	352	22.0	352	18.3	15
''	24.0	13.8	344	15.3	351	18.3	20
''	19.0	11.0	320	13.8	342	11.0	345
L/3	54.0	22.0	358	17.0	356	15.3	0
''	49.0	22.0	351	17.0	351	11.0	351
''	44.0	22.0	347	14.5	340	11.0	342

Contd.

Contd. Appendix A2

1	2	3	4	5	6	7	8
L/3	From inner wall towards outer wall	V	θ	V	θ	V	θ
''	39.0	21.0	342	13.8	336	11.0	336
''	29.0	15.3	340	9.8	336	9.8	335
''	24.0	11.0	327	11.0	325	11.0	323
''	19.0	11.0	326	11.0	324	11.0	322
L/2	54.0	21.0	26	20.0	21	18.3	21
''	49.0	18.3	4	11.0	355	18.3	39
''	44.0	22.0	26	23.5	21	18.3	41
''	39.0	22.0	21	21.0	21	21.0	28.5
''	29.0	15.3	43	21.0	22	20.0	31.0
''	25.0	15.3	38	18.3	30	18.3	28.0
''	19.0	17.0	51	15.3	51	18.3	43.0
2L/3	54.0	15.3	12	17.0	1	13.8	10
''	49.0	15.3	4	15.3	359	17.0	0
''	44.0	13.8	344	16.0	334	9.8	334
''	39.0	13.8	334	15.3	334	7.5	323

Contd.

Contd. Appendix A2

1	2	3	4	5	6	7	8
2L/3	From inner wall towards outer wall	V	θ	V	θ	V	θ
''	34.0	13.8	320	13.8	317	11.0	314
''	29.0	17.0	307	13.8	307	11.0	307
''	24.0	13.8	327	11.0	327	14.5	328
''	19.0	11.0	347	11.0	347	11.0	349
''	14.0	11.0	0	11.0	349	11.0	349
''	9.0	11.0	0	11.0	347	11.0	346
5L/6	54.0	17.0	0	17.0	0	15.3	0
''	49.0	15.3	6	15.3	359	17.0	2
''	44.0	13.8	0	15.3	359	11.0	357
''	39.0	13.8	0	13.8	0	11.0	357
''	29.0	11.0	2	11.0	356	11.0	353
''	19.0	11.0	354	11.0	356	11.0	1
''	14.0	11.0	15	11.0	5	11.0	5

Contd.

1	2	3	4	5	6	7	8
11L/2	From inner wall towards outer wall	V	θ	V	θ	V	θ
''	54.0	15.3	2	15.3	5	15.3	8.5
''	49.0	17.0	6	15.3	0	17.0	10
'''	44.0	15.3	354	15.3	1	17.0	6
''	34.0	15.3	356	15.3	356	17.0	8
''	24.0	13.8	357	13.8	357	15.3	4
''	19.0	11.0	352	11.0	352	11.0	0
''	14.0	9.8	350	9.8	356	11.0	357
''	9.0	7.5	356	7.5	352	11.0	351
Outlet (9cm away from inner wall)	U/S and D/S from inlet	V	θ	V	θ	V	θ
''	-15.0	24.6	332	23.5	340	24.6	349
''	-10.0	23.5	317	25.5	322	25.5	331
''	- 5.0	23.5	297	23.5	314	26.5	323
''	0	23.5	286	28.5	304	27.5	324
''	5	22.0	262	23.5	289	25.5	307
''	10	22.0	250	20.0	277	22.0	298
''	15	15.3	245	15.3	276	17.0	308

APPENDIX A3

d = 8.9 cm and F = 0.215

θ = direction fo flow in degrees as shown in Fig.6(a,b,c)

Section Inlet (9cm away from inner wall)	Distance in cm. in U/S and D/S direction from inlet	0.2d		0.4d		0.8d	
		V cm/sec.	θ in degrees	V cm/sec	θin degrees	V cm/sec.	θ in degree
1	2	3	4	5	6	7	8
''	-15.0	13.8	140	11.0	117	11.0	117
''	-10.0	27.5	86	30.5	86	40.0	90
''	- 5.0	27.5	83	30.5	83	38.2	89
''	0	30.0	81	31.25	85	43.0	89
''	5	23.5	79	29.0	81	38.0	90
''	10	30.0	76	33.5	80	40.0	90
''	15	30.5	75	35.0	78	37.0	83
L/12	From inner wall towards outer wall	V	θ	V	θ	V	θ
''	53.0	31.25	351	31.25	3	30.5	27
''	49.0	32.0	334	27.5	353	34.6	30
''	44.0	36.4	331	30.5	348	36.0	24
''	39.0	35.0	345	34.6	351	31.25	8

Contd.

Contd. Appendix A3

L/12	From inner wall towards outer one	V	θ	V	θ	V	θ
1	2	3	4	5	6	7	8
''	34.0	32.0	356	30.0	357	23.5	5
''	29.0	14.0	351	20.0	351	15.3	357
''	24.0	11.0	347	11.0	346	11.0	319
''	19.0	11.0	320	0	0	0	0
L/6	53.0	32.0	1	30.5	5	28.5	22
''	49.0	30.5	352	28.5	357	26.5	23
''	44.0	30.5	349	25.5	354	26.5	16
''	39.0	29.0	348	27.5	355	27.5	7
''	34.0	23.5	358	27.5	352	26.5	357
''	29.0	22.0	357	22.0	353	23.5	353
''	34.0	23.5	358	27.5	352	26.5	357
''	29.0	22.0	357	22.0	353	23.5	353
''	24.0	11.0	328	11.0	327	20.0	348
''	19.0	7.5	354	15.3	334	15.3	334

Contd.

Contd. Appendix A3

L/3	From inner wall towatds outer one	V	θ	V	θ	V	θ
1	2	3	4	5	6	7	8
L/3	53.0	18.3	0	21.0	358	18.3	1
''	49.0	18.3	354	18.3	352	18.3	0
''	44.0	18.3	355	18.3	352	17.0	358
''	34.0	15.3	353	15.3	350	18.3	351
''	29.0	11.0	342	11.0	338	11.0	339
''	24.0	11.0	346	11.0	334	11.0	338
''	19.0	13.8	325	9.8	314	11.0	327
''	14.0	15.3	310	13.8	301	11.0	320
L/2	53.0	20.0	13.	21.0	11	21.0	11
''	49.0	13.8	13	18.3	359	17.0	359
''	44.0	13.8	356	15.3	354	18.3	354
''	39.0	11.0	354	15.3	346	15.3	350
''	34.0	11.0	342	11.0	335	11.0	336
''	29.0	13.8	325	7.5	325	11.0	332
''	24.0	15.3	322	13.8	320	11.0	323
''	19.0	15.3	315	15.3	308	11.0	315
''	14.0	11.0	328	11.0	328	11.0	326
''	9.0	11.0	333	11.0	332	11.0	330

2L/3	From inner wall towards outer one	V	θ	V	θ	V	θ
1	2	3	4	5	6	7	8
2L/3	53.0	18.3	14	20.0	358	21.0	355
''	49.0	15.3	14	15.3	353	15.3	354
''	44.0	11.0	356	13.8	354	15.3	354
''	39.0	11.0	353	13.8	349	15.3	349
''	29.0	11.0	350	11.0	345	11.0	344
''	19.0	11.0	349	11.0	341	11.0	336
''	14.0	11.0	0	11.0	346	7.5	342
''	9.0	11.0	354	11.0	346	7.5	342

5L/6	From inner wall towards outer wall	V	θ	V	θ	V	θ
5L/6	53.0	11.0	2	15.3	356	15.3	351
''	49.0	15.3	353	15.3	353	18.3	348
''	44.0	15.3	355	18.3	352	18.3	349
''	39.0	15.3	349	15.3	349	18.3	349
''	29.0	15.3	32	17.0	22	18.3	15
''	19.0	15.3	25	15.3	25	17.0	17
''	14.0	15.3	30	11.0	22	15.3	5
''	9.0	15.3	23	15.3	17	17.0	12

Contd.

Contd. Appendix A3

11L/12	From inner wall towards outer one	V	θ	V	θ	V	θ
1	2	3	4	5	6	7	8
11L/12	53.0	15.3	0	15.3	0	17.0	359
"	49.0	15.3	2	15.3	1	18.3	357
"	44.0	18.3	10	17.0	0.0	20.0	4
"	39.0	15.3	8	15.3	5	17.0	2
"	34.0	15.3	7	17.0	3	18.3	1
"	24.0	15.3	8	11.0	6	13.8	354
"	19.0	15.3	10	15.3	349	17.0	349
"	14.0	15.3	12	15.3	10	15.3	359
"	9.0	11.0	17	17.0	5	15.3	0
Outlet (9 cm away from inner wall	U/S and D/S direction from outlet	V	θ	V	θ	V	θ
"	-15.0	15.3	329	21.0	324	22.0	326
"	-10.0	20.0	311	22.0	314	23.5	312
"	- 5.0	18.3	295	20.0	304	23.5	313
"	00	23.5	287	23.5	305	23.5	319
"	5	11.0	273	15.3	289	24.6	304
"	10.0	18.3	272	22.0	284	25.5	293
"	15.0	13.8	275	17.0	275	23.5	275